Technical Report No. 32-749

Evaluation of the Simulated Solar Spectrum in the JPL 25-ft Space Simulator

A. J. Drummond

J. R. Hickey

W. E. Schaefle

jpl

JET PROPULSION LABORATORY
CALIFORNIA INSTITUTE OF TECHNOLOGY
PASADENA, CALIFORNIA

August 31, 1965

NATIONAL AERONAUTICS AND SPACE ADMINISTRATION

Technical Report No. 32-749

Evaluation of the Simulated Solar Spectrum in the JPL 25-ft Space Simulator

A. J. Drummond

J. R. Hickey

W. E. Schaefle

George G. Goranson, Acting Manager
Space Simulators and
Facility Engineering Section

JET PROPULSION LABORATORY
CALIFORNIA INSTITUTE OF TECHNOLOGY
PASADENA, CALIFORNIA

August 31, 1965

CONTENTS

TABLES

TABLES (Cont'd)

FIGURES

FIGURES (Cont'd)

PREFACE

The work described in this Report was done by A. J. Drummond and
J. R. Hickey of the Eppley Laboratory, Inc., Newport, Rhode Island,
under JPL Contract DC4-31458 during October and November, 1964,
and is a continuation of the work begun in January, 1963, by them.
The report issued by the Eppley Laboratory on December 15, 1964, is
incorporated as Section II in a slightly altered version. The Appendixes
provide supplemental information regarding the study and are un-
abridged and unaltered copies of the original documents. Section I,
"Introduction," is provided by W. E. Schaefle.

ABSTRACT

35301

Detailed results of the Eppley Laboratory, Inc., spectral investigation of the solar simulation in the JPL 25-ft space simulator during October and November, 1964, are presented. The light source consisted of 133 2.5-kw mercury-xenon compact arc lamps. Two filter radiometers, a prism monochromator, and a grating monochromator were employed. Detailed results from both techniques are presented together with the correlation philosophy and results thereof. Agreement between the two methods is within ±4%. A comparison is made with the sunlight spectrum in space, and absorptances of some surface coatings under the two light sources are tabulated.

Author

I. INTRODUCTION

Section II of this Report consists of the results of an investigation of the solar simulation spectrum in the JPL 25-ft space simulator, data supplied to the Jet Propulsion Laboratory (JPL) by the Eppley Laboratory, Inc., of Newport, Rhode Island.

Two filter radiometers, one prism monochromator, and one grating monochromator were used in the investigation to evaluate the spectral character of the solar beam existing in the space simulator during October and November, 1964.[1] The filter-radiometer measurements, the monochromator measurements, and the correlation of the two techniques are presented, and the results are discussed. Fortran programs for the Jarrell–Ash (J–A)

and Perkin–Elmer (P–E) monochromator data and a Report of Calibration performed at the National Bureau of Standards on the spectral reflectance of two mirrors are included in the Appendixes. Also included is a copy of the interoffice memorandum by T. E. Gindorf, dated October 12, 1964, which is referred to at the beginning of the Eppley report (Section II).

Significant results are presented in brief, as follows.

A. Filter Measurements

No appreciable energy exists beyond 4μ, and approximately 1% exists beyond 2.2μ. The filter data for various filters are shown in the text in tabular form. A comparison of the percentage of irradiance in the chamber in wavelength bands with that occurring in similar wavelength bands in space is also given in tabular form. Changes in lamp input power from 2500 to 2000 w resulted in no

---

[1]The solar simulation system is described by H. N. Riise in "Modification of the Solar Simulation System of the JPL 25-ft Space Simulator," *Space Programs Summary No. 37-19, Vol. IV,* Jet Propulsion Laboratory, Pasadena, February 28, 1963, pp. 94–101.

significant variation in relative spectral emission over the wavelength examined, as seen in the test area, nor is there significant variation between air and vacuum measurements.

B. Monochromator Measurements

The spectral emission curves presented comprise the results of the monochromator investigation in air at Earth flux level and in vacuum at Earth and Mars flux levels. The data presented in these curves were integrated over bands to determine more accurate filter-factor numbers, and the percentage-of-total-energy values over the monochromator range for correlation with the filter-radiometer results.

There is a difference in spectra in the ultra-violet (UV) and visible (VIS) regions from that of an unmodified Hg-Xe arc. Some UV lines are of lower relative intensity due to transmission and reflection losses in the optical

system. Also time-dependent ozone absorption is indicated.

C. Correlation

Percentage-energy values for similar bands obtained by the two methods both inside (JC) and outside (JO) the chamber are presented in tabular form. For narrow-band filter-radiometer measurements, the agreement of percentage-of-total flux in the band with integrated-monochromator results is within 4% of the total energy. The repeatability of sets of data for similar conditions is good.

D. Spectral Comparison

The per unit absorptance for various materials in the band 0.25 to 2.0 μ under solar illumination and under the simulated spectrum in the 25-ft space simulator is presented in tabular form in Appendix E.

II. THE EPPLEY REPORT: SPECTRAL EVALUATION OF THE SOLAR SIMULATOR OF THE JPL 25-FT SPACE CHAMBER

A. General

During the period October 18–26, 1964, A. J. Drummond and J. R. Hickey of the Eppley Laboratory staff conducted a measurement program at JPL for the purpose of determining the spectral distribution of the energy in the solar simulator beam of the 25-ft space chamber. The test plan for these measurements was revised many times, and the final program was designated 25-45A. The tests described here were also discussed in a JPL Interoffice Memorandum.[2] During this test program, the Eppley personnel were aided by T. E. Gindorf, W. Schaefle, J. R. Gatewood, and J. Jolley. Engineers from JPL controlled the operation of the simulator facility. In addition to the authors of the Report, the following Eppley personnel participated in the very extensive effort involved in the data reduction: J. A. Garvey, W. J. Scholes, F. J. Griffin, and J. D. O'Brien.

As far as possible, tests were conducted in accordance with the aforementioned test plan and memorandum. Deviations are discussed in the appropriate sections of this Report. Many more filter-radiometer measurements were performed than were considered necessary for the fulfillment of the contract minimum requirement. The material presented here represents the first comprehensive examination of the relative and absolute spectral emission of this large solar simulator.

B. Filter-Radiometer Measurements

The radiometric method of ascertaining the spectral distribution of the emission of a source has been treated in detail by the present authors in reports to various organizations[3] (see Ref. 1). Essentially, the technique is one of exposing a calibrated nonwavelength-selective

---

[2]Interoffice Memorandum from T. E. Gindorf, dated October 12, 1964 (see App. D).

[3]General Electric Company, 1962–64; Jet Propulsion Laboratory, 1963; and NASA Lewis Research Center, 1963.

thermopile detector to the source the irradiance of which is under examination, and rotating a series of calibrated filters, in turn, in front of the detector. In the case of a filter that possesses the "ideal" rectangular-transmission characteristics, there is no difficulty in deriving the appropriate filter factor (to correct for reflection- and absorption-energy losses through the filter); it is simply the reciprocal of the main-band filter transmittance. Such filters have been designated broad bandpass filters in this Report.[4] On the other hand, where the filters designated here as narrow-bandpass filters have nonrectangular transmission characteristics, it is necessary to have some knowledge of the source-emission curve. In certain instances, it is sufficient to employ an accepted or assumed source curve based upon the general emission characteristics of the source type. Such generalized curves, however, are usually for an unmodified source.

In actuality, sources like those in solar simulators, sensitometers, and other complex systems, are modified spectrally by optical components; atmospheric absorption, especially by O_3, H_2O and CO_2, can also introduce (less marked) attenuation of the simulated beam at discrete wavelengths. In point of fact, in this specific examination, the principal source modifications occurred in the mercury-emission structure in the ultra-violet and low-visible regions, and as an increase in the level of the continuum in much of the source emission. The narrow-bandpass filter factors (originally derived by the planimeter method) were adjusted where necessary, mainly through consideration of the real-source curve as sampled by the standardizing broad-bandpass filters. In this portion of the investigation, it became apparent that, at least for a mercury-xenon source, the use of an electronic digital computer (involving application of an extended point-by-point method for filter-factor determination) resulted in improved accuracy of the filter factors in the mercury-emission regions, as well as substantial reduction in labor where many filters are concerned.

A total of 20 filter-radiometric runs were made, each series comprising measurements of total irradiance and measurements through 12 different filters. On the average, each measurement was repeated three or four times and, in cases of special interest, up to 10 times. Five filter wheels (four each carrying 12 narrow-bandpass filters and one carrying 12 broad-bandpass filters) were available. The total irradiance at the measurement plane was measured both at the commencement and at the termination of the filter runs.

Two sets of instrumentation were employed: an Eppley Mark-IV radiometer (JPL), and the first specimen of the new Eppley Mark-V radiometer (Eppley Laboratory), together with the associated remote control and readout components. The essential difference between the two detectors is the filter capability; the Mark-V carries two filter wheels, permitting a series of 24 filter measurements to be made without interruption, as compared with the 12-measurement series of the Mark-IV model. The latter generally carried narrow-bandpass filters and the former a combination of narrow- and broad-bandpass filters. Prior to this test program, both radiometers were equipped with the new, fast thermopile sensor recently developed at Newport. The rapid response of this unit (better than 1 sec for $1/e$ signal) in combination with fast readout (1-sec pen recorders) resulted in greatly improved precision and accuracy in the filter measurements (through reduction in emission effects owing to the short filter exposures now necessary). The high sampling speed of the system was an added advantage with regard to reduction in the time required for complete filter runs, despite many more (repeatable) exposures being made than was hitherto possible.

Fig. 1 shows the general experimental setup. The control and measurement equipment for the two radiometers is illustrated in Fig. 2, while Fig. 3 is a photograph of the radiometers, which were located inside the simulator during the test program.[5]

1. Apparatus

  a. Eppley Mark-IV radiometer, 6801-D(JPL)

  b. Eppley control console for (a) above, 2204(JPL)

  c. Leeds and Northrup dc-indicating amplifier for (a) above, LA41932(JPL)

  d. Leeds and Northrup Speedomax "H" Azar recording potentiometer for (a) above, LA48966 (JPL)

  e. Eppley Mark-V radiometer, 6812-D(Eppley)

  f. Eppley control console for (e) above, 2541(Eppley)

  g. Leeds and Northrup dc-indicating amplifier for (e) above, 1519413(Eppley)

  h. Leeds and Northrup Speedomax "H" Azar recording potentiometer for (e) above, LA48967(JPL)

  i. Eppley filter wheels Hg-, Carbon- and Xenon-arc series, and broad-bandpass series; 48 filters (Eppley)

  j. Eppley filter wheel Hg series; 12 filters (JPL)

---

[4]The UG-11 filter does not fall strictly into this category, but is so listed for convenience of distinction from the narrow-bandpass type.

[5]The photographs for Figs. 1, 2, and 4–6 were supplied by JPL. The photograph for Fig. 3 was taken at Newport.

k. Eppley dc-precision voltage reference for calibration of amplifiers and recorders, 701(Eppley)

l. Eppley Mark-I radiometers, 4384 and 5958, for monitoring of the simulated beam (JPL)

2. The Measurement Program

The number and type of radiometer-measurement series was dictated by the basic-monochromator evaluation program. The two radiometers were mounted on
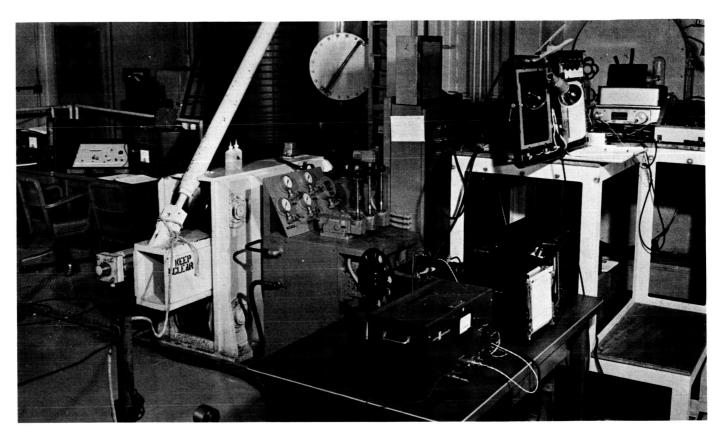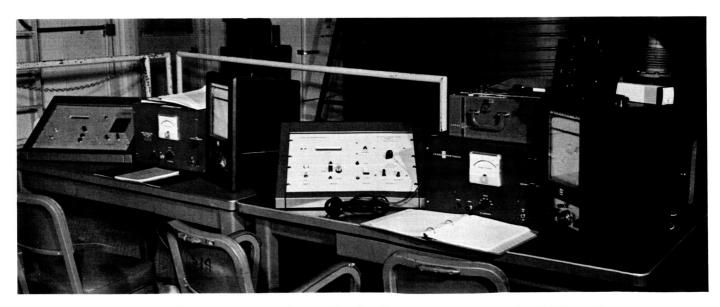

Fig. 1. General view of experimental setup

Fig. 2. Control and measurement equipment for the Mark-IV (left) and Mark-V (right) radiometers
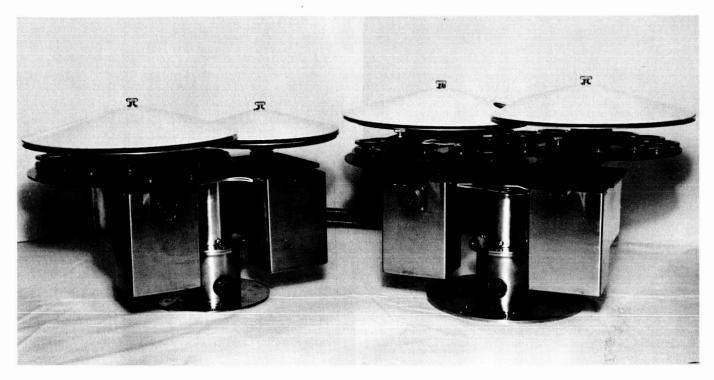
Fig. 3. The Mark-IV (left) and Mark-V (right) radiometers which were located inside the simulator during test program

rigid platforms inside the space chamber, near the center of the beam, 55 in. apart; as viewed from the chamber door, the Mark-IV instrument was positioned to the left of the Mark-V, the alignment being parallel to the door. One or the other of two Eppley Mark-I radiometers (JPL) were employed at various times to monitor the beam. The water-coolant temperature of the radiometer system was regularly monitored in the control room of the space chamber; $73 \pm 1°F$ was typical.

The sensitivities of the Mark-IV and -V radiometers are given in Table 1. Details of the 60 filters employed and their transmission characteristics are presented in Tables 2 and 3.[6] A total of 13 filter runs were obtained inside the chamber at atmospheric pressure, four runs under conditions of thermal vacuum (wall temperature $-270°F$; pressure 4.5×10^{-6} torr), and three runs outside the chamber at the position of monochromator reference lamp (to assist in the interpretation of the monochromator results). A summary of the measurement program is contained in Table 4.

[6]For further information about the shape of the transmission curves of these filters, and for a description of the radiometer calibration methods, consult the instruction manual, "Radiometers Marks III, IV and V: Description, Operation and Maintenance," Eppley Laboratory, 1964.

In the preliminary trials, it was noticed that the Mark-IV radiometer was indicating a total flux level about 6% higher than that derived from the Mark-V radiometer. Tests employing other detectors showed that there was a real difference of nearly 5% in irradiance between these two positions, in the same direction. This means that the two radiometers agreed in calibration to within $\pm1\%$, which is extremely satisfactory since they were calibrated independently, at Newport at different times, and were transported subsequently across the American continent. The Mark-I radiometers employed by JPL for monitoring of the beam intensity indicated flux values intermediate to those of the Mark-IV and -V instruments; but, in this instance, the radiometer calibration accuracy was not better than $\pm2\%$.

Table 1. Sensitivity of the Eppley Mark-IV and Mark-V radiometers employed in the JPL test program

Radiant flux level, w ft^{-2}	Mark, IV (6801-D), mv/w ft^{-2}		Mark, V (6812-D), mv/w ft^{-2}	
	Air	Vacuum	Air	Vacuum
1–150	0.0554	0.0720	0.0626	0.0840

Table 2. Narrow-bandpass filter characteristics

Filter series	Wavelength limits, $m\mu$	Filter factor	Filter series	Wavelength limits, $m\mu$	Filter factor
Hg (E)			Hg (JPL)		
1	265– 295	8.60	1	240– 300	11.1
2	275– 315	6.68	2	275– 315	5.72
3	300– 330	7.96	3	300– 335	8.73
4	—	—	4	—	—
5	355– 390	6.67	5	355– 390	6.01
6	390– 420	2.75	6	390– 420	2.57
7	415– 455	2.33	7	415– 455	2.22
8	515– 575	1.87	8	515– 575	1.64
9	565– 600	1.98	9	565– 600	1.83
10	600– 850	3.27	10	600– 850	3.10
11	800–1200	1.80	11	800–1200	2.06
12	1150–1900	1.78	12	1150–1900	1.70
Carbon			Xenon		
1	250– 300	10.8	1	—	—
2	295– 345	6.76	2	300– 350	11.0
3	345– 380	2.97	3	—	—
4	380– 420	1.85	4	385– 425	3.33
5	430– 505	3.97	5	430– 490	7.66
6	490– 600	2.18	6	525– 600	3.54
7	600– 700	2.21	7	620– 710	3.58
8	720– 840	3.83	8	710– 810	2.92
9	800– 980	4.14	9	770– 890	3.64
10	1020–1290	4.14	10	850–1070	3.67
11	1300–1800	4.02	11	1050–1600	2.82
12	1750–2600	2.81	12	1500–2200	2.70

Table 3. Broad-bandpass filter characteristics

Filter type	Center of lower cutoff, $m\mu$	Main-band transmission characteristics, $m\mu$[a]	Filter factor
1 Quartz	<250	0.91	1.10
2 WG 7	290	0.91	1.10
3 GG 22	390	0.88_5	1.13
4 GG 14	480	0.90	1.11
5 OG 1	535	0.90	1.11
6 OG 2	565	0.89_5	1.11_5
7 RG 1	605	0.90	1.11
8 RG 2	630	0.89_5	1.11_5
9 RG 5	665	0.90	1.11
10 RG 8	675	0.90	1.11
11 UG 11[b]	—	—	1.99
12 —			

[a] Average τ to 2500 $m\mu$.
[b] $\tau=0.05$ at 265 and 380 $m\mu$; $\tau=0.73$ at 325–330 $m\mu$.

Table 4. Series of radiometric measurements[a]

Run series	Radiometer	Monochromator run	Total flux, w ft^{-2}	Radiometer exposure	Run series	Chamber lamp	
						Number	Arrangement, w
1	Mark V	—	130		1–3	112	54: 2250
2	IV	Preliminary	141				58: 2500
3	V	—	130				
4	V	—	128		4–15	99	46: 2250
5	IV	MS1	139				53: 2500
6	V	—	128	Air inside chamber			
7	V	—	127				
8	V	—	129				
9	V	MS2	129				
10	IV	—	138				
11	V	—	127				
12	V	MS3	131				
13	V	—	131				
14	V	MS4	132				
15	IV	MS4	134				
16	IV	MS5	50	Thermal vacuum[a]	16	57	27: 2250 / 30: 2500
17	IV	MS6	51		17	57	57: 2000
18	IV	—	9	Air outside chamber at reference-lamp position	18–20	107	53: 2250 / 54: 2500
19	IV	—	9				
20	IV	—	9				

[a] Thermal vacuum conditions: wall temperature, −270°F; pressure, 4.5 × 10^{-6} torr.

The variable-aperture wheel incorporated in the Mark-IV-V design was next used to assess the extent of beam divergence at the positions of location of the Mark-IV and -V radiometers. (See Table 5).

length longer than about 4μ. This simple operation only involved exposure of the detector (in air) with and without the built-in removable crystal-quartz window in position. (See Table 6).

Table 5. Beam-divergence test

Aperture, deg	Recorder 1, deflection	Recorder 2, deflection
	Mark IV	Mark V
15	75.0	79.0
14	74.4	78.6
13	73.6	78.0
15	75.1	79.0
5	22.3	
15	75.0	

Table 6. Test for energy above 4μ

Quartz window	Recorder 1, deflection	Recorder 2, deflection
	Mark IV	Mark V
In	78.8	81.6
Out	86.8	90.6
In	78.8	81.7
Out	86.8	90.6
Ratio: in/out	0.91	0.90$_5$

Beam divergence (whole angle) of 15–16 deg is clearly indicated in both instances.

The next preliminary test was aimed at determining the proportion of radiation in the beam of the wave-

Since the transmission of a 2-mm-thick plane window of crystal quartz, over the integrated emission of the type of source under examination, is about 0.91–0.92, it was concluded that the source did not exhibit any measurable emission at wavelengths beyond 4μ, or so.

Table 7. Basic Mark-IV radiometric measurements[a]

Filter	Hg (JPL) filter, mμ	Run series, μv							Hg (E) filter, mμ	Run series, μv 19[d]	BB (E) filter, mμ	Run series, μv 20[d]
		2[b]	5[b]	10[b]	15[c]	16[c]	17[c]	18[d]				
1	240– 300	18.9	18.5	19.1	26.7	9.4	10.0	0.65	265– 295	0.80	>200	421
2	275– 315	57.2	53.2	55.4	65.5	23.8	24.3	1.95	275– 315	2.00	>290	415
3	300– 335	61.4	57.5	56.5	73.4	26.9	27.9	2.05	300– 330	1.75	>390	356
4	—	—	—	—	—	—	—	—	—	—	>480	315
5	355– 390	89.8	85.5	84.1	110	41.2	42.7	4.35	355– 390	4.70	>535	301
6	390– 420	113	108	107	142	54.0	53.3	5.80	390– 420	6.25	>565	272
7	415– 455	251	241	241	314	118	121	14.2	415– 455	14.3	>605	229
8	515– 575	371	366	362	444	170	172	22.8	515– 575	22.9	>630	225
9	565– 600	416	410	411	520	198	208	26.0	565– 600	26.4	>665	220
10	600– 850	219	220	219	265	102	98.0	13.4	600– 850	13.4	>675	218
11	800–1200	821	827	834	1013	381	384	52.6	800–1200	58.9	>265–380	29.3
12	1150–1900	878	886	893	1098	405	409	60.0	1150–1900	56.8	—	—
Total flux, mv	—	7.79	7.70	7.66	9.65	3.58	3.61	0.460	—	0.459	—	0.460

[a] Radiometer voltages before application of filter factors.
[b] Air, inside chamber.
[c] Thermal vacuum.
[d] Air, outside chamber.

Table 8. Basic Mark-V radiometric measurements[a]

Filter	Hg (E) filter, mμ	Run series, μv				C (E) filter, mμ	Run series, μv 11[b]	X (E) filter, mμ	Run series, μv 12[b]	BB (E) filter, mμ	Run series, mv				
		1[b]	4[b]	7[b]	8[b]						3[b]	6[b]	9[b]	13[b]	14[c]
1	265– 295	16.5	18.2	17.9	19.9	250– 300	21.4	—	—	>200	7.32	7.27	7.35	7.53	10.13
2	275– 315	50.0	50.5	51.0	52.3	295– 345	79.6	300– 350	47.7	>290	7.16	7.12	7.18	7.32	9.90
3	300– 330	49.4	47.8	48.4	48.2	345– 380	205	—	—	>390	5.86	5.90	5.96	6.00	8.15
4	—	—	—	—	—	380– 420	150	385– 425	81.5	>480	5.13	5.18	5.22	5.23	7.08
5	355– 390	86.9	84.3	86.3	88.6	430– 505	188	430– 490	81.7	>535	4.92	4.95	5.00	4.96	6.78
6	390– 420	110	111	112	115	490– 600	692	525– 600	387	>565	4.41	4.43	4.50	4.45	6.18
7	415– 455	235	231	233	231	600– 700	122	620– 710	92.4	>605	3.72	3.77	3.82	3.74	5.16
8	515– 575	368	363	—	362	720– 840	99.1	710– 810	69.5	>630	3.63	3.69	3.75	3.66	5.02
9	565– 600	425	419	417	421	800– 980	150	770– 890	62.9	>665	3.56	3.61	3.66	3.58	4.92
10	600– 850	212	216	218	218	1020–1290	286	850–1070	290	>675	3.51	3.56	3.62	3.54	4.89
11	800–1200	915	931	936	948	1300–1800	340	1050–1600	613	265–380	0.668	0.630	0.643	0.665	0.920
12	1150–1900	853	856	862	864	1750–2600	198	1500–2200	347	—	—	—	—	—	—
Total flux, mv	—	8.08	7.98	7.96	8.05	—	7.96	—	8.18	—	8.06	7.99	8.07	8.26	11.13

[a] Radiometer voltages before application of filter factors.
[b] Air, inside chamber.
[c] Thermal vacuum.

Each day, during the test period, the calibration of both recorders was established, using the Eppley precision voltage reference unit, and the scale values reset when necessary. The recorder accuracies throughout the program were thus maintained at ±0.2% of full-scale deflection, or better, throughout. The amplifiers were similarly checked at regular intervals.

3. Results

The results of the filter-radiometry aspect of the test program are presented in Tables 7–14. In the course of the investigation, it was found that filter 4 in both of the Hg series (E and JPL) was unsuitable because the peak transmission did not coincide with the main portion of

Table 9. Filtered radiometric data for Hg (E) and Hg (JPL) series[a]

		Hg (E)				
Filter	Region, mμ	Run series, air				
		1	4	7	8	Mean
1	265– 295	1.8	2.0	2.0	2.1	2.0
2	275– 315	4.2	4.2	4.3	4.3	4.2
3	300– 330	4.8	4.7	4.8	4.7	4.8
4	—	—	—	—	—	—
5	355– 390	7.1	7.0	7.2	7.3	7.1
6	390– 420	3.7	3.8	3.8	3.9	3.8
7	415– 455	6.8	6.8	6.8	6.7	6.8
8	515– 575	8.5	8.5	—	8.4	8.5
9	565– 600	10.4	10.4	10.4	10.4	10.4
10	600– 850	8.6	8.8	8.9	8.9	8.8
11	800–1200	20.4	21.0	21.1	21.2	20.9
12	1150–1900	18.8	19.1	19.2	19.1	19.1

		Hg (JPL)							
Filter	Region, mμ	Run series, air				Run series, vacuum			
		2	5	10	Mean	15	16	17	Mean
1	240– 300	2.6	2.7	2.7	2.7	3.1	3.0	3.1	3.1
2	275– 315	4.2	4.0	4.2	4.1	3.9	3.9	3.9	3.9
3	300– 335	6.9	6.6	6.5	6.7	6.7	6.6	6.7	6.7
4	—	—	—	—	—	—	—	—	—
5	355– 390	6.9	6.7	6.6	6.7	6.8	6.9	7.0	6.9
6	390– 420	3.7	3.6	3.6	3.6	3.7	3.9	3.9	3.8
7	415– 455	7.1	7.0	7.0	7.0	7.2	7.3	7.4	7.3
8	515– 575	8.0	8.0	7.9	8.0	7.7	7.9	7.9	7.8
9	565– 600	9.8	9.8	9.8	9.8	9.9	10.1	10.5	10.2
10	600– 850	8.7	8.9	8.9	8.8	8.5	8.8	8.4	8.6
11	800–1200	21.7	22.1	22.4	22.1	21.6	21.9	21.8	21.8
12	1150–1900	19.2	19.6	19.8	19.5	19.3	19.2	19.2	19.2

[a] All data expressed as percentage of total radiant flux after application of filter factors.

Table 10. Filtered radiometric data for C(E) and X(E) filter series[a]

C filter	Region, mμ	Run series, air 11	X filter	Region, mμ	Run series, air 12
1	250– 300	2.9	1	—	—
2	295– 345	6.8	2	300– 350	6.4
3	345– 380	7.6	3	—	—
4	380– 420	3.5	4	385– 425	3.3
5	430– 505	9.4	5	430– 490	7.7
6	490– 600	18.9	6	525– 600	16.7
7	600– 700	3.5	7	620– 710	4.0
8	720– 840	4.8	8	710– 810	2.5
9	800– 980	7.8	9	770– 890	2.8
10	1020–1290	14.9	10	850–1070	13.0
11	1300–1800	17.2	11	1050–1600	21.2
12	1750–2600	7.0	12	1500–2200	11.5

[a] Expressed as percentage of total radiant flux after application of filter factors.

Table 11. Filtered radiometric data for BB(E) filter series[a]

Filter	Region, mμ	Run series air					Vacuum
		3	6	9	13	Mean	14
1	>250	100.0	100.0	100.0	100.0	100.0	100.0
2	>290	97.8	97.9	97.9	97.8	97.9	97.7
3	>390	82.3	83.4	83.6	82.4	83.0	82.5
4	>480	70.7	71.9	72.0	70.6	71.3	70.7
5	>535	67.8	68.8	68.9	67.0	68.1	67.6
6	>565	61.1	61.8	62.1	60.3	61.3	61.9
7	>605	51.3	52.3	52.6	50.4	51.6	51.4
8	>630	50.3	51.4	51.8	49.6	50.7	50.3
9	>665	49.1	50.1	50.4	48.4	49.4	49.2
10	>675	48.3	49.3	49.7	47.7	48.7	48.5
11	265–380	16.4	15.8	15.9	16.1	16.1	16.5
12	—	—	—	—	—	—	—

Differential		Results					
1 − 2	<290	2.2	2.1	2.1	2.2	2.1	2.3
2 − 3	290–390	15.5	14.5	14.3	15.4	14.9	15.2
3 − 4	390–480	11.6	11.5	11.6	11.8	11.7	11.8
4 − 5	480–535	2.9	3.1	3.1	3.6	3.2	3.1
5 − 6	535–565	6.7	7.0	6.8	6.7	6.8	5.7
6 − 7	565–605	9.8	9.5	9.5	9.9	9.7	10.5
7 − 8	605–630	1.0	0.9	0.8	0.8	0.9	1.1
8 − 9	630–665	1.2	1.3	1.4	1.2	1.3	1.1
9 − 10	665–675	0.8	0.8	0.7	0.7	0.7	0.7
10 +	>675	48.3	49.3	49.7	47.7	48.7	48.5
11	265–380	—	—	—	—	—	—

[a] Expressed as percentage of total radiant flux after application of filter factors.

Table 12. Summary of filter measurements tabulated in Tables 9-11[a]

Narrow-band filters				Narrow-band filters			
Region, mμ	Air	Vacuum	Mean	Region, mμ	Air	Vacuum	Mean
240- 300	2.7	3.1	2.9	620- 710	4.0		4.0
250- 300	2.9			710- 810	2.5		2.5
265- 295	2.0		2.0	720- 840	4.8		4.8
275- 315	4.2		4.1	770- 890	2.8		2.8
275- 315	4.1	3.9		800- 980	7.8		7.8
295- 345	6.8		6.8	800-1200	20.9		21.6
300- 330	4.8		4.8	800-1200	22.1	21.8	
300- 335	6.7	6.7	6.6	850-1070	13.0		13.0
300- 350	6.4			1020-1290	14.9		14.9
345- 380	7.6		7.6	1050-1600	21.2		21.2
355- 390	7.1		6.9	1150-1900	19.1		19.3
355- 390	6.7	6.9		1150-1900	19.5	19.2	
380- 420	3.5			1300-1800	17.2		17.2
385- 425	3.3		3.6	1500-2200	11.5		11.5
390- 420	3.8			1750-2600	7.0		7.0
390- 420	3.6	3.8					
415- 455	6.8		7.0	Broad-band filters			
415- 455	7.0	7.3					
430- 490	7.7		7.7	<290	2.1	2.3	2.2
430- 505	9.4		9.4	290- 390	14.9	15.2	15.0
490- 600	18.9		18.9	390- 480	11.7	11.8	11.8
515- 575	8.5		8.1	480- 535	3.2	3.1	3.2
515- 575	8.0	7.8		535- 565	6.8	5.7	6.2
525- 600	16.7		16.7	565- 605	9.7	10.5	10.1
565- 600	10.4		10.1	605- 630	0.9	1.1	1.0
565- 600	9.8	10.2		630- 665	1.3	1.1	1.2
600- 700	3.5		3.5	665- 675	0.7	0.7	0.7
600- 850	8.8		8.7	>675	487	48.5	48.6
600- 850	8.8	8.6		265- 380	16.1	16.5	16.3

[a] Values expressed as percentage of total radiant flux.

the Hg-structured emission that this filter had been intended to isolate. In the xenon-arc filter series, filters 1 and 3 were likewise unsuitable. Of the broad-bandpass filters, 12 (KG 1) was not employed.

Tables 7 and 8 contain the basic-radiometric measurements as determined under the filters, but expressed in volts, uncorrected for the presence of the filter.

Tables 9-11 contain the filter-radiometer data, as corrected through application of the relevant filter factor and expressed as a percentage of the total irradiance. Combination of these figures with those of total irradiance (Table 4) will yield absolute values of spectral irradiance for the various wavelength intervals, if such information is desired. The high degree of filter-measurement repeatability will be apparent. Table 12 is a summary of the data included in Tables 9-11.

Table 13 has been prepared to demonstrate the excellent, mutual consistency between the different types of filter measurement summarized in Table 12. These figures provide an indication of the accuracy of the filter measurements; in general, they suggest that the individual values are reliable to better than ±5%.

In Table 14, the JPL solar-simulator values (expressed as percentage of total irradiance) are compared with those for corresponding wavelength intervals, according to the extraterrestrial spectral fluxes derived by Johnson (Ref. 2). Similar information is given for an average Johnson-Nicolet determination (Ref. 3). The intervals were selected for best coincidence with the Hg-structured emission, and for the filters or groups of filters available for this study. In the UV and VIS regions to 600mμ, the average interval is about 50mμ; from 600 to 1200mμ (NIR) it is 200mμ; then 400mμ to 1600mμ,

Table 13. Check on the mutual consistency of the filter measurements summarized in Table 12

| Narrow band vs broad band | | | |
NB region, mµ	Total, %	BB region, mµ	Total, %
250– 300	2.9	UG 11	16.3
300– 350	6.6		
345– 380	7.6		
350– 345	(−0.5)		
250– 380	16.6	265–380	16.3
265– 295	2.0	UG 11	16.3
295– 345	6.8		
345– 380	7.6		
265– 380	16.4	265–380	16.3
390– 420	3.8	GG 22	82.8
420– 430	(0.9)	−GG 14	−71.0
430– 490	7.7		
490– 480	(−0.7)		
390– 480	11.7	390–480	11.8
480– 490	(0.7)	GG 14	71.0
490– 600	18.9	−RG 1	−51.5
600– 605	(0.4)		
480– 605	20.0	480–605	19.5
535– 525	(−1.2)	OG 1	67.8
525– 600	16.7	−RG 1	−51.5
600– 605	(0.4)		
535– 605	15.9	535–605	16.3
565– 600	10.1	OG 2	61.6
600– 605	(0.4)	−RG 1	−51.5
565– 605	10.5	565–605	10.1
675– 710	(0.9)	RG 8	48.6
710– 810	2.5		
810– 800	(−0.4)		
800–1200	21.6		
1200–1300	3.0		
1300–1800	17.2		
1800–1750	(−1.5)		
1750–2600	7.0		

| Narrow band vs broad band | | | |
NB region mµ	Total, %	BB region, mµ	Total, %
675–2600	50.3	>675	48.6
770– 890	2.8	RG 8	48.6
850–1070	13.0	770–675	(−2.5)
890– 850	(−2.0)		
1050–1600	21.2		
1070–1050	(−0.5)		
1500–2200	11.5		
1600–1500	(−2.2)		
>2200	(0.5)		
>770	44.3	>770	46.1

| Narrow band vs narrow band | | | |
NB region, mµ	Total, %	NB region, mµ	Total, %
250–300	2.9	265–295	2.0
300–350	6.6	295–345	6.8
345–380	7.6	345–380	7.6
350–345	(−0.5)		
250–380	16.6	265–380	16.4
600–850	8.7	600–620	(0.9)
		620–710	4.0
		710–810	2.5
		810–850	(1.3)
600–850	8.7		8.7

| Broad band vs broad band | | | |
BB region, mµ	Total, %	BB region, mµ	Total, %
Q-WG 7	2.2	UG 11	16.3
WG 7-GG22	15.0		
390–380	(−1.0)		
<380	16.2	265–380	16.3

Table 14. Comparison between measured values of irradiance and extraterrestrial fluxes[a]

| Wavelength, mµ | Source | | |
| | JPL solar simulator | Sun | |
		Johnson	Johnson–Nicolet (average)
<300	2.9	1.2	1.0
300– 350	6.7	3.4	3.0
350– 390	7.5	3.5	3.1
390– 420	3.6	3.6	3.5
420– 460	7.0	5.8	5.6
460– 530	4.0	10.2	10.3
530– 560	6.2	4.2	4.2
560– 600	10.3	5.4	5.5
600– 800	6.8	20.8	21.2
800–1000	10.4	12.9	13.2
1000–1200	11.2	8.6	8.7
1200–1600	12.4	10.0	10.2

| Wavelength, mµ | Source | | |
| | JPL solar simulator | Sun | |
		Johnson	Johnson–Nicolet (average)
1600–2200	10.0	5.9	6.0
>2200	1.0	4.5	4.5
TOTAL	100.0	100.0	100.0
UV <380	16.5	7.2	6.4
VIS 380– 750	37.0	46.4	46.8
NIR >750	46.5	46.4	46.8

[a] Expressed as percentage of total.

11

$600m\mu$ to $2200m\mu$, and finally $>2200m\mu$. As in the case in Table 13, the monochromator curves were employed to equalize, as far as possible, the wavelength intervals being compared.

From a practical standpoint two important features of the tabular data are:

1. No significant variation in the relative spectral source emission, for vacuum exposure, with change in lamp input and output power over the ranges investigated;

2. No significant variation in the relative spectral source emission, between air and vacuum exposure, during the conditions of the test (i.e., relatively dry air with little dust–smog content).

These findings justified the combination of the data in average presentation, in Tables 9–14.

C. Monochromator Measurements

The monochromator-measurement program undertaken during this study consisted of many measurement sets and trials intended to show up differences in the spectral curve of the JPL solar simulator at various positions in the beam, in air, and for various intensity levels in vacuum. An outline of the tests is included in Table 15.

The monochromator tests of the JPL beam were performed using a dual monochromator method not previously used for the purpose of measuring energy in solar simulators. A high-resolution scan of the UV and VIS regions was performed with a J–A grating monochromator. The NIR region was measured using a P–E model-99 prism monochromator. This combination was chosen for ease of transport, based on size and possible damage conditions, flexibility, and the nature of the primary source; i.e., Hg-Xe arc lamps.

1. Apparatus

a. P–E model-99 monochromator No. 134 with quartz prism, and Reeder vacuum-thermocouple detector with quartz window

b. P–E control unit for automatic wavelength scan and chopper-regulation model 12-0111, No. 241

c. P–E amplifier unit model 81, No. 300

d. J–A monochromator ($180–800m\mu$) model 82–000, No. 376463 with automatic wavelength scan

e. Photomultiplier unit (Eppley unnumbered unit capable of attachment to model 99 or J–A monochromator with accommodation for most tubes, such as RCA 1P21, 1P28)

f. Photomultipliers: two 1P28, and one 1P21

g. Photomultiplier power supply: Furst-Electronics model 710P, No. 3189

h. General-Radio decade-resistance box for multipliers

i. Standards of spectral radiance (tungsten-strip lamps), EPT 1020 and EPT 1022 calibrated for spectral radiance over the range 0.25 to 2.5μ

j. Laboratory standard ammeter Sensitive Research Corporation Dynamometer model D, No. 945909 (accuracy 0.25%; range: 0–40 amps ac, 25 to 125 cps)

k. Mirrors (common to beam and standard): two flat front-surfaced aluminum on pyrex; one spherical front-surfaced aluminum on pyrex with 27-cm radius of curvature

l. Leeds and Northrup Speedomax "G" recording potentiometer, B-63-44595-2-1 (JPL)

m. Filters:

  1. Order suppression for grating instrument: Corning 9-54, Pyrex, 3-70, 3-75, 3-68 and Schott RG 5

  2. For stray energy elimination in P–E model 99: Corning 3-68

  3. For linearity checking: Thin Films Products inconel-on-quartz neutral-density filters, with the following specified transmittance at $550m\mu$: 0.70, 0.40, 0.30, 0.10, 0.03, 0.01, 0.003 and 0.001

  4. Holmium-oxide filter for wavelength calibration

n. Control circuit for standard lamps: two Variacs, one filament transformer, one 10-to-1 power transformer, and one stabilization transformer

o. Eppley type-A standard-lamp mounting fixture

p. Small Hanovia mercury-lamp unit for wavelength calibrations

q. Miscellaneous items used only in trial experiments: Eppley laboratory-type thermopile, No. 5556 with filter wheel; two small diffusing spheres[7]

2. Theory of Measurement

The basic theory of this type of measurement has been reported elsewhere (Refs. 1 and 4). The use of the standards of spectral radiance is also well documented

---

[7]Except where otherwise indicated, the items listed above were supplied by Eppley Laboratory.

Table 15. List of monochromator tests by measurement series

MS series	Trial	Source	Mono-chromator	Conditions and explanation	MS series	Trial	Source	Mono-chromator	Conditions and explanation
1	(1)	EPT 1022	99	Preliminary checks to establish range of 99		(3)	EPT 1020	J–A	Standard for trial 4
	(2)	EPT 1022	99	Calibration using HoO filter		(4)	Chamber-beam mirror in center	J–A	Earth solar constant; air (window in and out during run)
	(3)	EPT 1020 EPT 1022	99	Check of standard agreement		(5)	EPT 1020	J–A	Rerun of trial 3
	(4)	Chamber-beam mirror 18 in. back from center	99	Earth solar constant; air, (window in) exploratory		(6)	EPT 1020	J–A	Standard for trial 7
						(7)	Chamber-beam mirror in center	—	Earth solar constant; air (window in)
	(5)	Repeat of trial 4 for record				*			Check of shape of 546-mμ Hg line using filter A8 at J–A entrance slit to determine if the unexpected profile is caused by stray
	(6)	EPT 1020	99	Standard run for correlation with trial 5	4	(1)	EPT 1020	J–A	Standard for trial 2
	*			Unnumbered trials for calibration of J–A mono-chromator and determination of mesaurement settings		(2)	Chamber beam	J–A	Earth solar constant; vacuum
						(3)	EPT 1020	99	Standard for trial 4
						(4)	Chamber beam	99	Earth solar constant; vacuum
	(7)	EPT 1020	J–A	Standard run for correlation with trial 8	5	(1)	EPT 1020	J–A	Standard for trial 2, 2(a)
	(8)	Chamber-beam mirror 18 in. back from center	—	Earth solar constant; air (window in)		(2)	Chamber beam (partial scan)	J–A	Mars solar constant by reducing number of lamps; vacuum (window fogging experienced)
2	(1)	EPT 1020	—	Standard for trial 2		(2a)	Chamber beam	J–A	Repeat of trial 2 after window cleaning
	(2)	Chamber-beam mirror 18 in. forward from center	—	Earth solar constant; air (window in)		(3)	Chamber beam	99	Mars solar constant; vacuum
	(3)	EPT 1020	J–A	Rerun of trial 1 to check repeatability of lamp positioning and phototube stability		(4)	EPT 1020	99	Standard for trial 3 and for MS6, trial 2
	(4)	EPT 1020	99	Standard for trial 5	6	(1)	Not run; same as MS5, trial 4		
	(5)	Chamber beam	99	Earth solar constant; air (window in)		(2)	Chamber beam	99	Mars solar constant by reducing lamp-input power; vacuum
3	(1)	EPT 1020	99	Standard for trial 2		(3)	EPT 1020	J–A	Standard for trial 4
	(2)	Chamber-beam mirror in center	99	Earth solar constant; air, 2 scans superimposed on chart (window in, green ink; window out red ink)		(4)	Chamber beam	J–A	Mars solar constant by reducing lamp power; vacuum

(Ref. 5).[8] These references have been made available to JPL personnel previously, and many discussions on their content preceded this undertaking. However, certain basic points should be repeated here, and the differences caused by the change in monochromator systems from those previously discussed should be explained.

Use of the standards of spectral radiance is primarily to eliminate the necessity of determining the spectral throughput of the monochromator system and the relative spectral response of the detector employed in the monochromator. The absolute values of spectral radiance are not used explicitly in this type of study. The source curves obtained by the ratio method using these standards is termed the relative-spectral-emission curve rather than the relative spectral-radiance curve. This curve of the source under test has relative meaning insofar as the integral of the spectral-emission curve, over a wavelength band at least 10 times the bandwidth of the instrument, is related to the total integrated emission in proper proportion. In some instances, the actual data points have absolute meaning. These instances are usually restricted to emission sources having a continuous spectrum, near-continuous spectrum, or band emission for which the natural bandwidth is large as compared with the monochromator bandwidth.

It is well known that many bandwidth-corrective procedures can be applied. These corrections usually constitute an unnecessary complication, because only integral values are desired. The monochromator can produce meaningful integral results for narrow bands, as will be discussed later. Usually the source is not compatible with the standard, insofar as it may not be uniform, in either spectral distribution or total radiance, over the area or solid angle to which the standard's usage is restricted by calibration procedure. Also, for the type of study reported here, values of absolute irradiance, at a position remote from the monochromator, are of primary interest. This explanation does not imply that absolute values of spectral radiance cannot be obtained by using such standards, but that the conditions for this are highly restrictive and, as pointed out, unnecessary.

All absolute values of irradiance are obtained experimentally, employing the filter-radiometric technique, as described previously in this Report.

The main purpose of the monochromator study is to obtain curves of relative spectral emission for determining filter factors for radiometer measurements and to produce a source curve. As a by-product of this attempt, integrated relative-emission values may be obtained for smaller wavelength bands than are possible with the radiometer method. Resolution limitations must be borne in mind for this type of analysis. The discussion is especially applicable to measurements in which the monochromator has a varying bandwidth with wavelength.

Based on the philosophy presented above, the relative emission curve is said to be that for a position in space considered as the source. This position corresponds to that occupied by the usable area of the filament of the reference lamp during the standardization. Figure 4 shows the standard lamp in position at JPL.[9] This Figure also shows the required mirror arrangement for the use of spectral-radiance standards. The spherical mirror is mounted on the laboratory stand to the right, just in front of the brass photomultiplier housing on the J–A monochromator. The permanent, flat mirror is mounted on the stand to the left. The back of the second flat mirror is visible just behind the spherical mirror. This mirror was only used during the P–E model-99 runs.

The image of the filament can be seen at the entrance slit of model 99. Figure 5 shows the monochromator arrangement during the measurement of the chamber beam. The beam appears bluish and is incident on the model 99. The model-99 slits are filled, as can be seen by the visible reflections from the slit jaws.

---

[9]The location of the filament is that for which the JO curves, mentioned later, will apply.
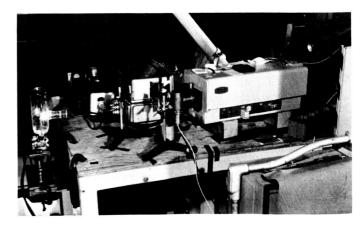
Fig. 4. Measuring arrangement of monochromator during a standard (tungsten-in-quartz) lamp calibration run

---

[8]"Instructions for Using Standards of Spectral Radiance," Eppley Laboratory reprint of NBS circular, revised February, 1961, is available from the Eppley Laboratory.
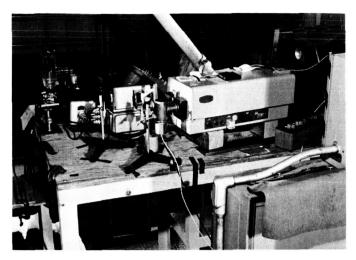
Fig. 5. Measuring arrangement of monochromator during a chamber-beam run

To obtain the JO curve from the data, the ratio of the corrected output reading for the unknown to the corrected output reading for the standard is multiplied by the value of spectral radiance of the standard for each specified wavelength of interest.[10] The relative emission curve of the solar beam inside the chamber (JC) is obtained by correcting the JO curve for the reflectance of the redirecting mirror and for the transmittance of the quartz window in the chamber door. The theory of filter factors and integrated values will be discussed in the next Section.

For reasons previously mentioned, the monochromators chosen for this task were the model 99, with quartz prism, and the J–A (Ebert) monochromator with a 30,000 lines/in. grating. At the outset of the measurement program, it was intended to test both monochromators for use with diffusing spheres, in order to reduce errors that might be caused by source nonuniformity. However, during the initial tests, it was determined that this method would create problems, which will be described below, and the end results of the monochromator determinations are proof that little would have been gained by employing the spheres.

3. Method

a. Positioning and usage of monochromators. The positioning of the monochromators was based on the compatibility of the working area with the requirements of the standard-lamp positioning, the space available, and

the ease and speed of operation. A well-constructed work table was supplied by JPL for the placement of the Eppley equipment. The table was extremely stable and was designed in such a way as to assure accessibility to all components. This table was placed in front of the chamber door (see Figs. 1, 4, 5, and 6). The standard-lamp mounting bracket attached to the table (Fig. 4) proved to be highly satisfactory.

The reasons for the final placement of the monochromators on the table and for dispensing with the diffusing spheres were based on (1) geometry factors; (2) ease and speed of operation for many repetitive scans; and (3) small output signal over some spectral regions with the diffusers in place. These considerations are all interrelated.

With the diffusers mounted on the instruments, it would have been necessary to arrange the reference mirrors for the standard lamps in a manner deviating from that prescribed. A slight deviation was needed to avoid contact of the spherical mirror with the photomultiplier housing or the J–A instrument. Also, if an alternate position were chosen, this same housing would have blocked the beam to the model 99. Since one of the monochromators would require three mirrors in its input optics, and, since mirrors of this type have a more adverse effect on the UV than on the NIR region, the model chosen for the three-mirror arrangement was 99.

Based on the signal outputs of the two instruments and the resolution characteristics, together with the detector availability and the expressed desire of JPL to have more detailed results in the UV–VIS region, it was decided to use the J–A instrument for the lower wavelengths and the model 99 for the NIR. The only alternative to this procedure, under the circumstances, would have been to realign the mirror system after every trial of each measurement set.

b. Methods of test. The measurement series of Table 15 show the order in which tests were performed. For each chamber-beam run, at least one standard run was accomplished. The ability of the system to reproduce the calibration of one standard, considering the other to be known, was within the limitations of the standards; viz., about $\pm 4\%$ from 250 to $290m\mu$, $\pm 2\%$ from 290 to $500m\mu$ and $\pm 1\%$ from $500m\mu$ to 2.6μ.

The final readout for both monochromators was a Leeds and Northrup Speedomax "G" recorder set at 10-mv full

---

[10]For further discussion on this matter, see subsection "Data Reduction and Results," item 4 of this Section.
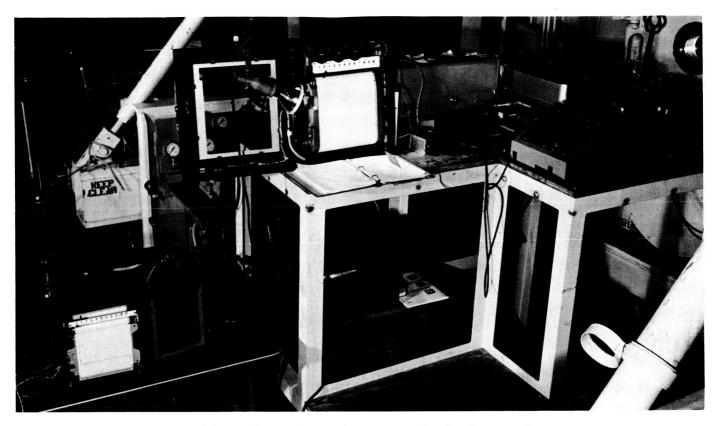
Fig. 6. View of the readout and control instrumentation for the monochromator runs

scale (see Fig. 6). The J–A-instrument's detector was an RCA 1P28 photomultiplier with the General-Radio decade-resistance box as load. The millivolt output across the resistance was plotted on the recorder as a function of wavelength in a linear manner, because the automatic wavelength scan was set at 250 Å/min and the recorder at 6 in./min, yielding a readout resolution of 41.7 Å/in. of chart. The load resistance was varied during the scans to get the best signals over the range of the blocking filter used (see discussion below). The model-99 output was also read on the same recorder, as a linear function of drum number. The drum-number-to-wavelength conversion is logarithmic. A curve of calibration in terms of drum number vs wavelength was previously supplied to JPL. Instruction manuals for both monochromators have also been made available to JPL. The output of the model 99 was varied over the range of test by changing the amplifier-gain setting. A study (at the Eppley Laboratory) of the characteristics of the amplifier has shown that the amplifier steps increase the output reading by 1.6^n, where n is the gain setting designation. These points will be discussed again in connection with data breakdown.

During scans with the model-99 monochromator, a Corning 3-68 (yellow glass) filter was placed at the entrance slit to eliminate any short-wavelength stray radiation below the monochromator-overlap region, which consists here chiefly of the green line and yellow doublet of mercury emission. A set of blocking filters to prevent interference of higher orders was used with the J–A instrument. The filters used, with the corresponding limits of the scan are as follows: Corning 9-54, 2500 to 3000 Å; pyrex, 3000 to 4000 Å; Corning 3-75, 4000 to 5000 Å; Corning 3-70, 5000 to 5500 Å; Corning 3-68, beyond 5500 Å.

c. Calibrations. In addition to the standard-lamp checks previously mentioned, the wavelength scales of both monochromators were checked using a small mercury lamp. The model-99 wavelength scale was fitted to the calibration curve by adjusting the Littrow mirror. The J–A instrument was found to be within the manufacturer's specifications and was not altered. Cautions regarding backlash effects and scanning-speed errors as described in the instruction manual were adhered to. Using an NBS Holmium-oxide filter, the wavelengths of the specified absorption peaks were checked with the tungsten-filament lamp as source. Agreement in this case was within the resolution capabilities of the instrument.

d. Resolution. After consideration of the overlap problem for the monochromators, coupled with the low output from the model-99 monochromator, the slits were set at 0.5 mm for the model 99 and 200µ for the J–A. The resolution of each system is best interpreted by studying the final curves. The resolution is fixed for the grating instrument and varies with wavelength for the prism instrument. Detailed analysis of this point has not been undertaken, since integral solutions over large bandwidths are of interest in correlation.

4. Data Reduction and Results

a. General. All data reduction was handled by computer methods. Two different programs were used to obtain the relative emission curves, one for each monochromator. These differed only slightly in the equation for obtaining JO. The most important consideration in choosing data points for the spectral emission curves is the wavelength selection. Looking ahead to the final integration process, it will be realized that with a curve such as mercury emission, a program using the trapezoidal rule will be the least complicated. Therefore, successive wavelength points should be chosen such that the line connecting their ordinate values in the final curve will be straight. Any discontinuities in the data curves of the source, the window-transmittance curve, the mirror-reflectance curve, and the interference-filter transmittance curve (JPL Hg for use with the Mark-IV radiometer), or any regions of continuously varying slope, must be carefully scrutinized.

For each monochromator, a set of master data at these selected wavelengths is given in Appendixes A and B. Appendix A contains the master data for the J–A region, and Appendix B that for the model 99. Other curves than the JO curve are required for each spectral scan. The product function (PFO) curve for each interference-filter region is also of interest for determination of the filter factor at the reference position (lamp-filament position). The JC curve is the most important curve, because it is the spectral distribution inside the space chamber. This curve is the JO curve modified by the transmittance of the quartz window in the chamber door, and by the reflection of the mirror inside the chamber. All other mirrors and filters used do not enter the calculations because they are common to both the standard-lamp run and the chamber-beam run for any measurement set. The last curve obtained is the PFC curve, which is the product-function curve inside the chamber. The product-function curves PFO and PFC were determined for the JPL-Hg series filters only, although many other filters were used in the radiometer determinations. Broad-

band filters need no such analysis of their product functions. The window-transmittance and mirror-reflectance values will be discussed later.

Only one integration program is needed, because both spectral emission programs produce output data in the same format.

b. Spectral emission-curve programs. The master data in Appendixes A and B consist of all the information common to any given wavelength, for all measurement sets, with the same monochromator over the range of a given interference filter. It occupies columns 1 through 32 on the computer data sheets and on the input cards. These data include wavelength (W), reflectance of the mirror (RM), transmittance of the window (TQ), spectral radiance of the standard (VS), filter number (FN) and filter transmittance (TFX). There are four variables remaining to be printed on the data sheet. The millivolt readings for the chamber beam (DU) and those for the standard (DS) are included for both monochromators. The other data needed for the J–A runs are the resistance across the multiplier, designated RS for the standard trials and RU for the chamber-beam trials. The other data needed for the model-99 runs are the amplifier-gain settings, designated AS for the standard trials and AU for the chamber-beam trials. The equations necessary to accomplish the data reduction are included in the programs and need not be discussed here (see Tables 16 and 17).

For the J–A data, a print-out of the photomultiplier current is included in the output. The output cards of both programs serve as input cards for the integration program.

Assumed decimal-point positions were used in all fields for the master data and the additional data. No decimal points appear on the data sheets. The letter x in any variable name should be ignored because it is inserted for format compatibility only.

c. Spectral emission-curve results. The curves for each monochromator for each measurement set comprise the results.

Due to the small difference in the curves from set to set, it is not considered necessary to present all the curves in this Report. Those of measurement-set 1 for JC and JO are given in Figs. 7, 8, 9 and 10. These curves show the differences for air measurements outside and inside the chamber. The JC curves for measurement-set 4 are given in Figs. 11 and 12. These show the Earth

Table 16. Jarrell–Ash data for JPL chamber[a]

```
JPL PROGRAM NUMBER 1
JARRELL-ASH DATA FOR JPL CHAMBER
J. R. HICKEY - EPPLEY LAB.
STATE-      C  FOR COMMENT
 MENT
  NO.
   1   567 10   15    20    25    30    35    40    45    50    55    60    65    7072

        C      ANALYSIS OF THE SPECTRUM OF THE JPL SOLAR SIMULATOR - JA MONO DATA
               PRINT 1
             1 FORMAT(1H ,45HSPECTRAL EMISSION USING JA MONOCHROMATOR)
               PRINT 2
             2 FORMAT(1H ,56HDATA INCLUDES SPECTRAL EMISSION AT MEASUREMENT PLANE
               1JO)
               PRINT 3
             3 FORMAT(1H ,65H PRODUCT FUNCTIONS AT MEAS.PLANE,PFO,EMISSION CURVE
               1OF CHAMBER JC)
               PRINT 4
             4 FORMAT(1H ,58HPRODUCT FUNCTIONS FOR CHAMBER,PFC,AS FUNCTION OF W
               1AND FN)
               PRINT 5
             5 FORMAT(1H ,51HINCL.PHOTOMULTIPLIER CURRENTS DURING RUN   CS AND CU)
               PRINT 6
             6 FORMAT(1H ,71H  W    FN    JO         PFO        JC        PFC
               1    CS           CU)
           100 READ10,  W,RM,TQ,VS,FN,TFX,DU,DS,RU,RS
            10 FORMAT(F5.1,2F5.3,E9.2,F3.0,3F5.3,2F5.0)
               CS=DS/RS
               CU=DU/RU
               XJO=VS*(CU/CS)
               XJC=XJO/(TQ*RM)
               PFO=XJO*TFX
               PFC=XJC*TFX
               PRINT20,  W,FN,XJO,PFO,XJC,PFC,CS,CU
            20 FORMAT(F6.1,1X,F4.0,1X,4E10.4,1X,F12.7,1X,F12.7)
               PUNCH30,  W,FN,XJO,PFO,XJC,PFC
            30 FORMAT(F6.1,1X,F4.D,1X,4E10.4)
               GO TO 100
               END
         PARAMI9R1010
```

Table 17. Model-99 data for JPL chamber[a]

```
JPL PROGRAM NUMBER 2
MODEL-99 DATA FOR JPL CHAMBER
J. R. HICKEY - EPPLEY LAB.
STATE-      C  FOR COMMENT
 MENT
  NO.
   1   567 10   15    20    25    30    35    40    45    50    55    60    65    7072

        C      ANALYSIS OF THE SPECTRUM OF THE JPL SOLAR SIMULATOR - MOD 99 DATA
               PRINT1
             1 FORMAT(1H ,51HSPECTRAL EMISSION USING MODEL 99 MONOCHROMATOR        )
               PRINT2
             2 FORMAT(1H ,56HDATA INCLUDES SPECTRAL EMISSION AT MEASUREMENT PLANE
               1JO)
               PRINT3
             3 FORMAT(1H ,65HPRODUCT FUNCTIONS AT MEAS.PLANE,PFO,EMISSION CURVE
               1OF CHAMBER JC)
               PRINT4
             4 FORMAT(1H ,58HPRODUCT FUNCTIONS FOR CHAMBER,PFC,AS FUNCTION OF W
               AND FN)
               PRINT5
             5 FORMAT(1H ,  H  W    FN     JO         PFO        JC        PFC   )
           100 READ10,  W,RM,TQ,VS,FN,TFX,DU,DS,AU,AS
            10 FORMAT(F5.1,2F5.3,E9.2,F3.0,3F5.3,F3.0,F5.0)
               XJO=(VS*DU*1.6**(AS-AU))/DS
               XJC=XJO/(TQ*RM)
               PFO=XJO*TFX
               PFC=XJC*TFX
               PRINT20,  W,FN,XJO,PFO,XJC,PFC
            20 FORMAT(F7.1,1X,F4.0,1X,4E10.4)
               PUNCH30,  W,FN,XJO,PFO,XJC,PFC
            30 FORMAT(F6.1,1X,F4.0,1X,4E10.4)
               GO TO 100
               END
         PARAMI9R1010
```
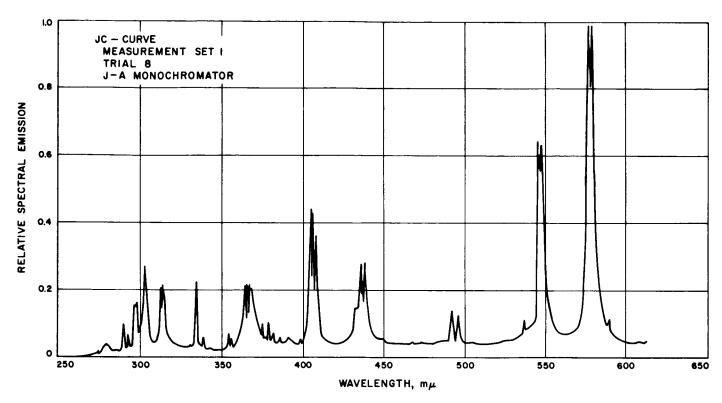
Fig. 7. The UV and VIS relative emission curve representative of the JPL solar simulator at the Earth solar-constant flux level, in air (JC)
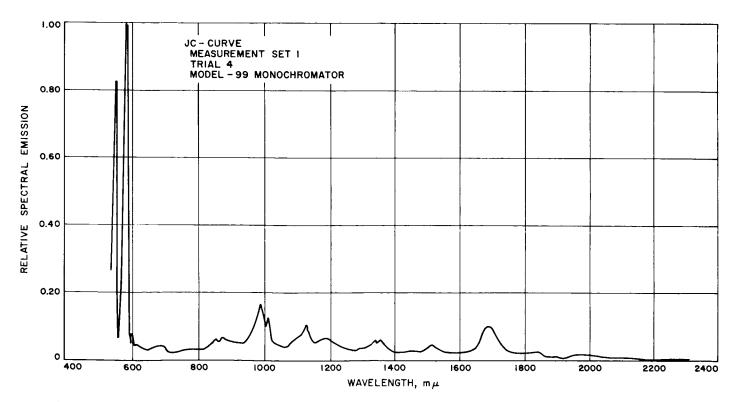
Fig. 8. The NIR relative emission curve representative of the JPL solar simulator at the Earth solar-constant flux level, in air (JC)
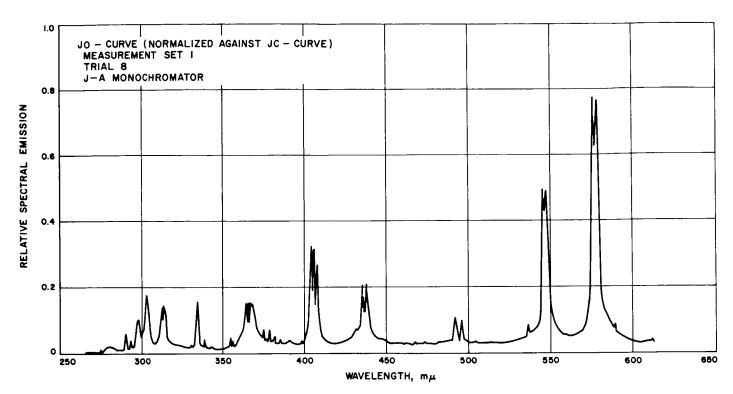
Fig. 9. The UV and VIS relative emission curve representative of the JPL solar simulator at the Earth solar-constant flux level, in air (JO)
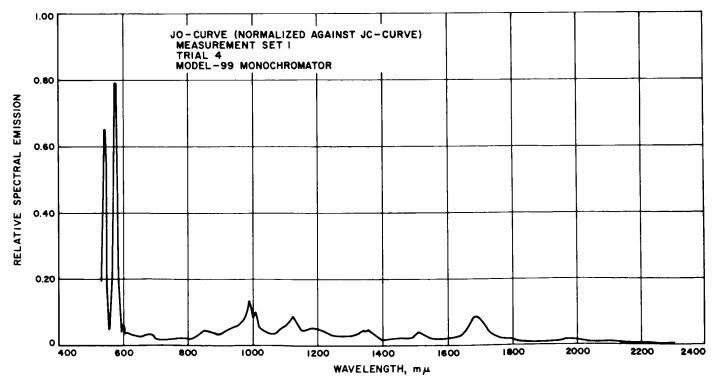
Fig. 10. The NIR relative emission curve representative of the JPL solar simulator at the Earth solar-constant flux level, in air (JO)
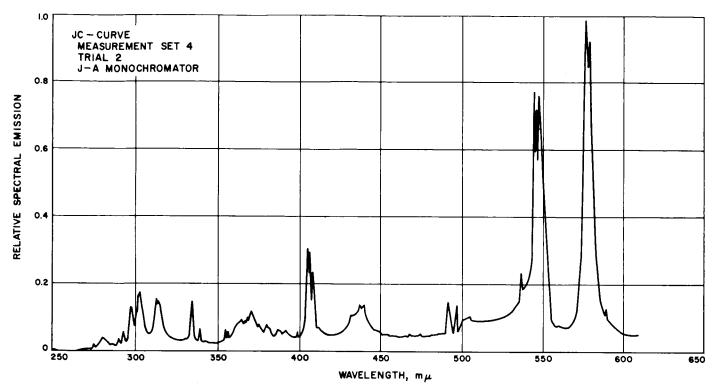
Fig. 11. The UV and VIS relative emission curve representative of the JPL solar simulator at the Earth solar-constant flux level, in vacuum (JC)
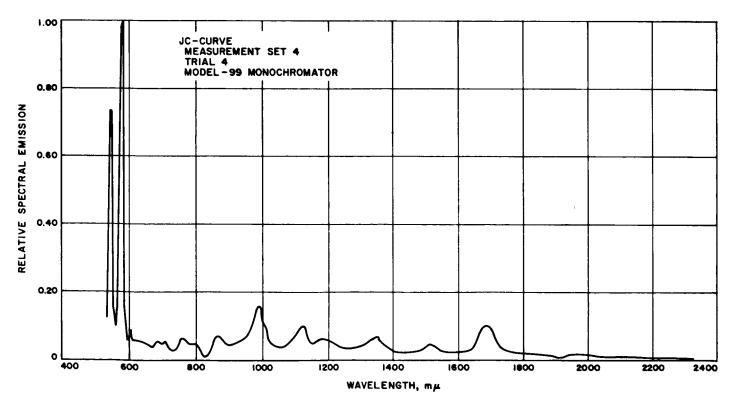
Fig. 12. The NIR relative emission curve representative of the JPL solar simulator at the Earth solar-constant flux level, in vacuum (JC)

solar-constant beam in vacuum. The reduced lamp-power curves for vacuum at the Mars solar-constant level are shown in Figs. 13 and 14. These are from measurement-set 6. The other Earth solar-constant air curves are similar to MS1. The Mars solar-constant curves of MS5 are similar to the curves of MS4. The similarity of the curves is confirmed in the radiometer results (see Tables 9–11).

The curves are plotted with maximum ordinate normalized to 1.00, with the exception of the JO curve of MS1 that was normalized to the maximum ordinate of the JC curve for MS1. The wavelength-scale interval differs from J–A to model-99 data.

d. Integration program. The integration program (see Table 18) was operated using the output cards of the other programs as input data. The program separately integrates all four output variables as a function of wavelength and prints out the incremental and total values of each up to the specified wavelength. Each filter region

Table 18. Computer program: Integration of emission

```
JPL PROGRAM NUMBER 3
INTEGRATION OF EMISSION
J. R. HICKEY - EPPLEY LAB.
STATE-      C FOR COMMENT
MENT
NO.
  1   567 10   15   20   25   30   35   40   45   50   55   60   65   7072

    C     INTEGRATION FOR FILTER FACTORS, FORMAT FROM JPL CHAMBER STUDY
          PRINT1
        1 FORMAT(1H ,69HFILTER FACTOR INTEGRATION PROGRAM USING FORMATS FROM
          1JPL CHAMBER JOB)
          PRINT2
        2 FORMAT(1H ,69H      AA           AB           AC           AD
          1CUMULATIVE OFFSET)
          READ40, W,FN,XJO,PFO,XJC,PFC
       40 FORMAT(F6.1,1X,F4.0,1X,4E10.4)
          AAAA=0
          ABBB=0
          ACCC=0
          ADDD=0
      600 WW=W
          XJOO=XJO
          PFOO=PFO
          XJCC=XJC
          PFCC=PFC
          AAA=AAAA
          ABB=ABBB
          ACC=ACCC
          ADD=ADDD
          READ40, W,FN,XJO,PFO,XJC,PFC
          AA=((XJOO+XJO)*(WW-W))/2.
          AB=((PFOO+PFO)*(WW-W))/2.
          AC=((XJCC+XJC)*(WW-W))/2.
          AD=((PFCC+PFC)*(WW-W))/2.
          PRINT5,WW,W,FN
        5 FORMAT(2X,F8.1,2X,F8.1,2X,F5.1)
          PRINT50,AA,AB,AC,AD
       50 FORMAT(2X,E10.4,2X,E10.4,2X,E10.4,2X,E10.4)
          AAAA=AAA+AA
          ABBB=ABB+AB
          ACCC=ACC+AC
          ADDD=ADD+AD
          PRINT60,AAAA,ABBB,ACCC,ADDD
       60 FORMAT(20X,E10.4,2X,E10.4,2X,E10.4
          GO TO 600
          END
    PARAMI9R1010
```
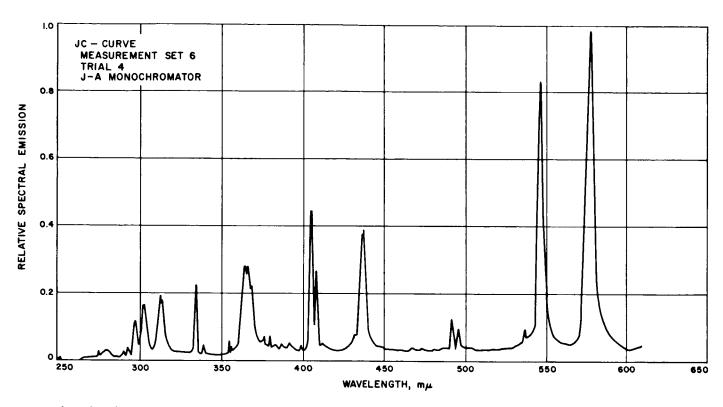
Fig. 13. The UV and VIS relative emission curve representative of the JPL solar simulator at the Mars solar-constant flux level (by reduction of lamp input power), in vacuum (JC)
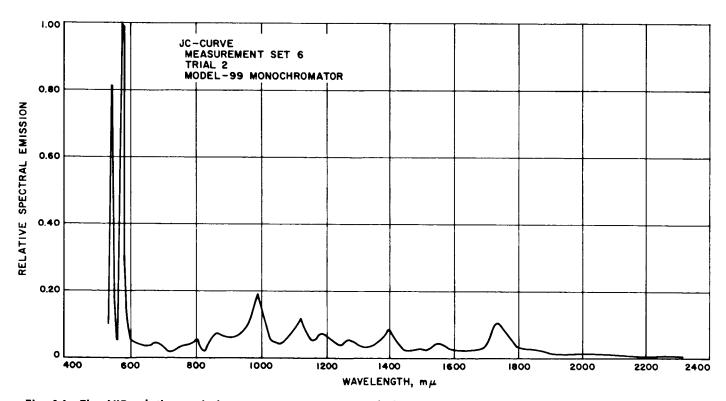
Fig. 14. The NIR relative emission curve representative of the JPL solar simulator at the Mars solar-constant flux level (by reduction of lamp input power), in vacuum (JC)

was run separately with the program given here. This type of output facilitates the determination of filter factors and their practical limits. The output data consist of integrated values of spectral emission for JO(AA) and JC(AC), and also the integrated product functions of PFO(AB) and PFC(AD). The filter regions for the initial analysis are the 0.001-τ(transmittance) limits of the given filter. The print-out includes FN. Incremental

values are printed on one line of each output print, and cumulative values are offset, on the next, in the order AA, AB, AC, AD. All integrations were performed using the trapezoidal rule as previously stated.

e. Integration results. The results of the integration program can be applied for two purposes. First, they are the basis for the determination of filter factors. The final limits chosen for a given filter may not necessarily be the 0.001-transmittance limits of that filter. If the filter factor decreases rapidly as the limits are narrowed, it is obvious that the overall range chosen for integration was too large. It must be remembered that the filter factors obtained in this way are correct for those limits chosen. However, the percentage of energy at the radiometer receiver between the originally programmed and the finally adopted wavelength limits may be less than 1% of the total. Thus, the final limits are more representative of the actual situation. Let us say that the first result of the integration is a means of setting filter-factor limits. Table 19 gives an example of such an analysis.

Table 20 gives the 0.001-τ filter factors for the JPL-Hg filters. The second function of the integration program is

Table 19. Change of filter factor with change of limits for filter A5 using MS1 results[a]

Band limits, mμ	Filter factor, JO and PFO	Total integral PFO, %	Filter factor, JC and PFC	Total integral PFC, %
345 –397	8.59	100.0	8.59	100.0
350 –397	8.37	99.9	8.37	99.9
354.2–397	7.99	99.6	7.98	99.6
355.0–397	7.91	99.5	7.90	99.5
355.0–395	7.72	99.5	7.73	99.5
355.0–390	7.34	98.8	7.34	98.8

[a] The original 0.001-τ limits are 345–397mμ, and the radiometer limits are 355–390 mμ.

Table 20. Filter factors at 0.001-τ limits[a]

Filter	Monochromator	0.001-τ band limits, mμ	Air JC	Air JO	Vacuum JC	Vacuum JO	Vacuum, reduced power JC	Vacuum, reduced power JO
1	J–A	245.0–315.8	51.5	56.7	48.1	53.4	55.6	62.2
2		268.0–320.0	9.36	9.44	9.39	9.53	10.5	10.6
3		286.0–345.0	11.9	11.8	11.2	11.3	10.8	10.7
4[b]		320.0–364.5	20.4	20.5	19.4	19.4	12.5	12.7
5		345.0–397.0	8.60	8.59	9.92	9.91	8.09	8.09
6		380.0–429.0	3.60	3.59	4.18	4.18	3.71	3.70
7		407.7–463.3	3.23	3.23	3.36	3.36	2.86	2.85
8		504.6–588.7	3.68	3.69	3.32	3.32	3.65	3.66
9		555.0–608.0	2.37	2.37	2.42	2.42	2.34	2.34
10	P–E 99	587.0–955.0	6.05	6.12	5.07	5.14	6.43	6.52
11[c]		670.0–1900	3.98	4.01	4.27	4.28	3.92	3.94
12[c]		1008–2097	2.39	2.39	2.39	2.39	2.38	2.40

[a] MS1, MS4, and MS6 monochromator results (JPL filters)

[b] Not used for radiometer results.

[c] Includes secondary transmission regions.

to produce values of percentage-of-total energy over the monochromator range. No absolute values of irradiance are inferred from the integration program except where the integrals are related to radiometer determinations.

f. Transmittance and reflectance data. The effects of transmittance of the quartz window, mounted in the chamber door, and the spherical mirror used to direct the beam out through this port, can be seen by examining the JO and JC curves of MS1. As stated previously, the curves differ only by these two factors. The RM and TQ values inserted as part of the master data were determined separately, prior to the performance of these tests. These two variables probably introduce the largest errors in the measurement in the UV and low VIS ranges.

An attempt to determine the actual TQ values was made during the tests, as can be seen in Table 15. The method involved monochromator determinations of spectral distribution with the quartz window in and out of the beam port. Initial analysis of these results showed it to be impractical. In the case of the model-99 analysis, the values were in fair agreement with those obtained independently by spectrophotometer examination of the actual window. For the J–A region, the values were too high at the wavelength of maximum deflections to be credible. The high values are most likely caused by the change of the image-plane position due to the change in the optical-path length resulting from the use of such a thick sheet of quartz (⅝-in. thickness). The small slit and high resolution of the J–A instrument, combined with the fact that only the ordinate values at peaks were acceptable for analysis, accounts for the inability to obtain meaningful results over that region. The values used for TQ are those obtained using the P–E Spectracord 4000 spectrophotometer at the Eppley Laboratory.

The reflectance values of the mirror were determined using a sample flat mirror deposited at the same time as the actual spherical-mirror deposition. This sample mirror, along with another that was not considered because of a smudge on the surface, was sent to the U.S. National Bureau of Standards for a reflectance determination. A copy of the report of this examination is included in Appendix C. As will be noticed, no absolute values of reflectance are given in this Report. Recorder charts of the reflectances of the two samples vs that of MgO were supplied. Also, no values of the reflectance of MgO were given. It was necessary, therefore, to arrive at the reflectance values (included in the master data) based on these ratios and the MgO values of Sanders and Middleton

(Refs. 6 and 7). These references contain a large amount of data on MgO reflectance. The particular data, from which the reflectance of the mirror was calculated, consist of a combination of those for freshly deposited MgO over the various spectral regions discussed here ($\sim$0.25 to 2.3μ).

The effects of these undesirable methods of obtaining the reflectance and transmittance functions is primarily noticed in the ultra-violet and lower-visible regions. This is due to the fact that both the functions are fairly constant over the range beyond the low visible, with some notable exceptions in the absorption bands of aluminum (near 800mμ) and of the quartz (near 1.4μ and 2.2μ). Other problems with these values are caused by the mismatching of the data at the so-called overlap positions of the reflectometers and spectrophotometer. These errors are caused by the changes in detector geometry and resolutions of the instruments in the NIR from those in the UV and VIS regions. Based on these factors and the recommendation of NBS (see App. C), all data were corrected to the NIR values.

g. Interpretation of spectra. The curves as depicted in Figs. 7 through 14 show the characteristic mercury-arc emission as anticipated. Some of the mercury line structures exhibit a different appearance than would be the case for an unmodified arc. The primary differences are apparent in the J–A region. Some UV lines are of lower relative intensity because of the adverse effects of the transmittance and reflectance of optical components of the solar simulator. Other unexpected absorptions, which are obvious in the source curves, seem to be caused by ozone. It would appear that this ozone absorption occurs in the lamp compartment above the space chamber, and it appears to be variable with time. A comparison of the results of MS1 vs MS6 shows how the line shapes were altered through this effect. At one time, there was suspicion of photocell nonlinearity at some of the stronger emission regions. However, a thorough check of the output-current values on the computer print-out sheets dispelled this suspicion.

As drawn, it is considered that the curves are representative of the chamber beam under the specified conditions. Some doubt as to the validity of the line shapes near 360 and 440mμ of Fig. 11 has arisen. It is believed that an error in scale reading from the original data was introduced. It is also believed that such errors will not greatly affect the integral values. These data will be re-examined and significant changes, if any, will be reported.

D. Correlation of Monochromator and Filter-Radiometer Data

The correlation of the two measurement techniques is based essentially on the agreement of integrated monochromator data with the final radiometer data. The use of the monochromator data in determining filter factors was mentioned previously in this Report. The discussion that follows is intended to show that accurate resolution corrections are not necessary when reducing values in wide spectral bands.

The results reported here are the first, to the best of our knowledge, that have been obtained using two monochromators varying so widely in their characteristics. It will be recalled that absolute values of irradiance were derived using the unfiltered radiometer, and all other results are given as percentages of that total irradiance. The correlation in this Section is based on MS1 results.

1. Overlapping of the Monochromators

Under the specified measuring conditions, the only practical overlap region was that including the mercury green line and yellow doublet. This is roughly the region from 530 to 608mμ. Based on the consideration that the higher-resolution instrument is more appropriate for this structured region, it was decided to prove overlap reliability by defining the J–A region as the wavelengths below 604mμ and the model-99 region as the region beyond 604mμ. This wavelength corresponds within 1mμ, in a very flat unstructured region, with the center of cutoff of the RG1 filter in the broad-bandpass set. Partition of the spectrum into two large regions is thus possible in such a way as to permit evaluation of the two total-integral-monochromator values. Table 21 shows the agreement of total-integral values obtained by the radiometer and by the monochromator method for JC and JO of MS1. The broad-band measurements, made outside the chamber (RS20), were considered appropriate for this analysis. RS6 data were used for JC comparison. The agreement of the JO data is perfect, while the agreement of the JC data shows a difference of only 1% of total energy.

2. Analysis of the Filter Bands

Two series of filters will be discussed here: the broad-band filters and the JPL-Hg filters. The analysis is presented for MS1 only. All other measurement sets can be treated in the same manner. Both JO and JC integrals are included. Table 22 gives the integrated broad-band results and comparison with the radiometer results for

Table 21. Monochromator separation agreement with RG1 filter separation[a]

Item	Outside chamber, units	Inside chamber, units
Total integral	9477.9	12227.2
J–A integral	4246.6	5714.8
Model-99 integral	5231.3	6512.4
Percentage below 604mμ		
Radiometer	44.8	47.7
J–A monochromator	44.8	46.7
Percentage beyond 604mμ		
Radiometer	55.2	52.3
Model-99 monochromator	55.2	53.3

[a] MS1, RS6, and RS20 series (see Tables 3, 4, 7, 8 and 11).

Table 22. Correlation of JO integration with radiometer results for broad-bandpass filters[a]

BB(E) filter	Bandpass region, mμ	Integral value	Percentage of total flux — Monochromator	Percentage of total flux — Radiometer
1	>200	9477.9	100.0	100.0
2	>290	9426.8	99.5	98.5
3	>390	8480.1	89.5	86.7
4	>480	7545.3	79.6	76.1
5	>535	7125.5	75.1	72.6
6	>565	6405.3	67.6	65.9
7	>605	5231.3	55.2	55.2
8	>630	5149.9	54.3	54.5
9	>665	5045.2	53.2	53.1
10	>675	5011.8	52.9	52.5
Differential Results				
1 — 2	<290	—	0.5	1.5
2 — 3	290–390	—	10.0	11.8
3 — 4	390–480	—	9.9	10.6
4 — 5	480–535	—	4.5	3.5
5 — 6	535–565	—	7.5	6.7
6 — 7	565–605	—	12.4	10.7
7 — 8	605–630	—	0.9	0.7
8 — 9	630–665	—	1.1	1.4
9 — 10	665–675	—	0.3	0.6
10+	>675	—	52.9	52.5

[a] MS1 and RS20 series (see Table 7).

the JO integration. It is obvious from the broad-band results that over these large integration limits agreement of the two methods to within 4% of the total energy is possible, and that, in general, the agreement is much better. The largest departure differentially is 1.8% of the total radiation.

The same type of analysis for the JC curve is given in Table 23. The agreement of the broad-band results is not as good as that for the integral JO curve. The maximum error is 9.5% of total flux for the region beyond 480mμ, 3.5% of which is caused by the basic JO data, and the remainder is most likely caused by errors in the assumed throughput, which will be discussed later.

Table 24 presents the analysis of the agreement between monochromator and radiometer results for narrow-bandpass filters (JPL Hg). This table is based on the JO

Table 23. Correlation of JC integration with radiometer results for broad-bandpass filters[a]

BB(E) filter	Bandpass region, mμ	Integral value	Percentage of total flux	
			Monochromator	Radiometer
1	>200	12227.2	100.0	100.0
2	>290	12138.4	99.3	97.9
3	>390	10773.4	88.1	83.4
4	>480	9989.7	81.4	71.9
5	>535	9442.2	77.2	68.8
6	>565	8507.5	69.6	61.8
7	>605	6512.4	53.3	52.3
8	>630	6410.3	52.4	51.4
9	>665	6278.6	51.3	50.1
10	>675	6236.4	51.0	49.3
Differential Results				
	<290	—	0.7	2.1
	290–390	—	11.2	14.5
	390–480	—	6.7	11.5
	480–535	—	4.2	3.1
	535–565	—	7.6	7.0
	565–605	—	16.3	9.5
	605–630	—	0.9	0.9
	630–665	—	1.1	1.3
	665–675	—	0.3	0.8
	>675	—	49.0	49.3

[a] MS1 and RS6 series (see Tables 8 and 11).

Table 24. Correlation of JO integration with radiometer results for narrow-bandpass filters[a]

Hg(JPL) filter	Bandpass region, mμ	Integral value	Percentage of total flux	
			Monochromator	Radiometer
1	240–300	141.5	1.5	1.65
2	275–315	375.7	4.0	2.4
3	300–335	381.1	4.0	3.9
4	320–364.5	277.1	2.9	—
5	355–390	400.2	4.2	5.7
6	390–420	402.8	4.2	3.3
7	415–455	417.4	4.4	6.9
8	515–575	1105.0	11.7	8.2
9	565–600	{1145.0(J–A) / 1187.4(99)}	{12.1(J–A) / 12.5(99)}	10.3
10	600–850	662.6	7.0	9.0
11	800–1200	2226.1	23.5	23.5
12	1150–1900	2469.4	26.0	22.2
Total	>200	9477.9	100.0	100.0

[a] MS1 and RS18 series (see Table 7).

Table 25. Correlation of JC integration with radiometer results for narrow-bandpass filters[a]

Hg(JPL) filter	Bandpass region, mμ	Integral values	Percentage of total flux	
			Monochromator	Radiometer
1	240–300	229.6	1.9	2.7
2	275–315	576.1	4.7	4.0
3	300–335	564.1	4.6	6.6
4	320–364.5	391.8	3.2	—
5	355–390	545.5	4.5	6.7
6	390–420	549.0	4.5	3.6
7	415–455	560.9	4.6	7.0
8	515–575	1434.0	11.7	8.0
9	565–600	{1481.0(J–A) / 1492.8(99)}	{12.1(J–A) / 12.2(99)}	9.8
10	600–850	893.3	7.3	8.9
11	800–1200	2728.6	22.3	22.1
12	1150–1900	2912.4	23.8	19.6
Total	>200	12227.2	100.0	100.0

[a] MS1 and RS5 series (see Tables 7 and 9).

curves of MS1. The agreement for the region of filter 9 is given for both J–A and model-99 data, showing again the overlap agreement of the monochromators.

Table 25 is the equivalent of Table 24 for the JC curve analysis of MS1. The results of Tables 24 and 25 show that agreement for narrow bands of the order of 4% or less is possible.[11] The errors in agreement between monochromator and radiometer results should be the same for the JO integrals and the JC integrals, since the latter are obtained from the same basic data as the former. The differences in agreement can only be explained by examining the intervening media, as will be described in the next subsection.

3. Throughput Corrections

The major source of error in the monochromator-to-radiometer correlation of the JC integrals seems to be the existence of unknown attenuation of the chamber beam. The overall effect of absorption, reflection, and transmission phenomena may be considered together as "throughput." As mentioned previously, the system throughput depends on the beam-attenuation processes, occurring between the position of the radiometer inside the chamber and the position of the monochromator-measurement plane. In the integrated-monochromator results, this throughput has been assumed and inserted into the program as RM and TQ. Either of these may contain errors, especially in the low-wavelength regions. No absorption functions for CO_2, H_2O vapor or O_3 were included. In the case of radiometer measurements, geometry also becomes a throughput factor.

In considering a series of filters, a band throughput can be postulated for each filter region. For example, the overall assumed throughput for the monochromator results is the total-integrated JO value divided by the total-integrated JC value (9477.9/12227.2) or 0.775. The total measured throughput for the radiometer data is the ratio of the total output signals outside and inside the chamber (0.460/7.70) or 0.0597. The effect of geometry is obvious here. Considering the geometry effect to be a constant spectrally (which is not strictly valid in the regions where scattering occurs), an attempt can be made at determining the throughput errors inherent in the assumed throughput data. Table 26 gives the throughput values for the bands of the JPL-Hg filters. Correction of the monochromator-integral values may be made, to a first approximation, by multiplying the JC-band integrals (including the total integral) by the (A/M) ratios of Table 26.

---

[11]Compare Table 28 where these results are also presented.

Table 26. System throughput data[a]

Hg (JPL) filter	Band throughput		
	Measured, M	Assumed, A	Ratio, A/M
1	0.0351	0.616	17.5
2	0.0356	0.652	17.8
3	0.0356	0.676	19.0
4	–	–	–
5	0.0509	0.734	14.4
6	0.0537	0.734	13.7
7	0.0589	0.744	12.6
8	0.0623	0.771	12.4
9	0.0634	$\begin{cases} 0.773(J{-}A) \\ 0.795(99) \end{cases}$	$\begin{cases} 12.2(J{-}A) \\ 12.5(99) \end{cases}$
10	0.0609	0.746	12.2
11	0.0636	0.816	12.8
12	0.0677	0.848	12.5
Total	0.0597	0.775	13.0

[a] MS1, RS5 and RS18 series.

Adjusted monochromator results are obtained by determining the new percentages of total based on these new integral values.

The same effect would be achieved by dividing the JO integrals by the ratios of the radiometer-band outputs to total output. Thus, Table 26 is included only for demonstration purposes. If no errors in the assumed-band throughput were made, the A/M ratio would be a constant. The fact that it is not necessitates an investigation of possible correction. It should be mentioned here that the radiometer-output values (actual μv signals) are considered to be correct to a higher accuracy than necessary for this procedure to be valid.

Table 27 contains data related to the first approximation corrections. The adjusted-integral values have meaning only when used to determine percentage of total flux. In this table, the new monochromator percentages are correlated with the unmodified radiometer-determined percentages. It must be remembered that errors in spectral throughput affect the JC-curve shape. Any change in the JC-curve shape may change the filter factors, which then will cause changes in the radiometer-derived percentages. The application of this type of higher-order corrections is not included, because it is believed that the JC errors are approaching the errors inherent in JO. Table 28 shows this correlation.

Broad-bandpass filters do not need as extensive a correction process, because their filter factors are virtually unchanged by changes of the shape of the source curve.

Table 27. Agreement in percentages in bands after first-order throughput corrections[a]

Hg(JPL) filter	Bandpass region, mμ	Adjusted integral value	Percentage of total flux	
			Monochromator	Radiometer
1	240–300	4018.0	2.5	2.7
2	275–315	10254.6	6.5	4.0
3	300–335	6783.6	4.3	6.6
5	355–390	7855.2	4.9	6.7
6	390–420	7521.3	4.7	3.6
7	415–455	7067.3	4.4	7.0
8	515–575	17781.6	11.2	8.2
9	565–600	{ 18068.2(J–A) 18660.0(99)	{ 11.4(J–A) 11.7(99)	9.8
10	600–850	10898.3	6.9	8.9
11	800–1200	34926.1	22.0	22.1
12	1150–1900	36405.0	22.9	19.6
Total	>200	158953.6	100.0	100.0

[a] JC integrals of MS1 series.

Table 28. Change in agreement of narrow-band results[a]

Hg(JPL) filter	Basic JO	Differences of total flux radiometer minus monochromator, %	
		JC before correction	JC after correction
1	+0.1$_s$	+0.8	+0.2
2	−1.6	−0.7	−2.5
3	−0.1	+2.0	+2.3
5	+1.5	+2.2	+1.8
6	−0.9	−0.9	−1.1
7	+2.5	+2.4	+2.6
8	−3.5	−3.7	−3.0
9	{ −1.8(J–A) −2.2(99)	{ −1.3(J–A) −1.4(99)	{ −1.6(J–A) −1.9(99)
10	+2.0	+1.6	+2.0
11	0.0	−0.2	−0.1
12	−3.8	−4.2	−3.3

[a] Throughput corrections for the JC integrals.

The correction consists of one approximation only. Table 29 shows the results of this correction. The small differences between basic JO agreement and corrected JC data are the very small radiometer errors. Based on this agreement, it has been shown that the integral values of irradiance for various filter bands can be obtained for the chamber beam to the same percentage error as for the beam at the measurement plane, within the limits of the instruments used to obtain measured throughput values.

Table 29. Change in agreement of broad-bandpass results[a]

BB(E) filter	Measured-band throughput	Corrected percentage of total	Difference of total flux radiometer minus monochromator,[b] %		
			Basic JO	Basic JC	JC corrected
1	0.0579	100.0	0.0	0.0	0.0
2	0.0583	98.9	−1.0	−1.4	−1.0
3	0.0604	85.7	−2.8	−4.7	−2.4
4	0.0609	75.6	−3.5	−9.5	−3.7
5	0.0609	71.5	−2.8	−8.4	−2.7
6	0.0614	63.7	−1.7	−7.8	−1.9
7	0.0607	52.6	0.0	−1.0	−0.3
8	0.0610	51.5	+0.2	−1.0	−0.1
9	0.0610	50.4	−0.1	−1.2	−0.3
10	0.0613	49.9	−0.4	−1.7	−0.6
Total	0.0575	100.0	—	—	—

[a] Throughput corrections to JC integrals.
[b] See Tables 22 and 23.

4. Summary of Correlation

All absolute values of irradiance are obtained from radiometer measurements. The filter factors used to allow interpretation of these measurements are obtained from a source curve derived by monochromator methods. Every integral value of irradiance within a filter band is dependent on both techniques. The values given in Section II, subsection B of this Report comprise the test results. In Section II, subsection D, the agreement of the integral values of the monochromator curves with the radiometer values has been shown. It should be stressed that there is no need for repeated monochromator testing, unless deviations from the radiometer results, presented here, are encountered during routine measurements.

REFERENCES

1. Hickey, J. R., and A. J. Drummond, "The Measurement of Simulated Solar Radiation with Special Reference to Spectral Determination," *Vide* (in press).

2. Johnson, F. S., "The Solar Constant," *Journal of Meteorology*, 11, 431–439, 1954.

3. Nicolét, M., "Sur la détermination du flux énergétique du rayonnement extra-terrestre du soleil," *Archiv für Meteorologie, Geophysik und Bioklimatologie, Series A. Meteorologie und Geophysik*, 3, 209–219, 1951.

4. Hickey, J. R., W. J. Scholes, and A. J. Drummond, "On a Method of Examining the Spectral Emission Properties of High-Pressure Compact Arc Lamps," *Applied Optics* (in press).

5. Stair, R., R. G. Johnston, and E. W. Halbach, "Standard of Spectral Radiance for the Region of 0.25 to 2.6 Microns," *Journal of Research of the National Bureau of Standards—Section A, Physics and Chemistry*, 4, 291–296, 1960.

6. Middleton, W. E. K., and C. L. Saunders, "Absolute Spectral Diffuse Reflectance of Magnesium Oxide," *Journal of the Optical Society of America*, 41, 6, 419–24, 1951.

7. Saunders, C. L., and W. E. K. Middleton, "Absolute Spectral Diffuse Reflectance of Magnesium Oxide in the Near Infrared," *Journal of the Optical Society of America*, 43, 1, 58, 1953.

APPENDIX A
Master Data for Jarrell—Ash Monochromator

FORTRAN CODING FORM

IBM

Page 1 of 14

Program: APPENDIX A   MASTER DATA FOR JARREL ASH
Programmer: SEE PROGRAM 1   Date: 5 NOV 64

Punching Instructions — Graphic / Punch — Card Form #

Identification (73–80)

C FOR COMMENT

STATEMENT NUMBER	RM	TQ	VS	FN	TF
2330	230	835	2.55E+03	1	.001
2340	250	837	2.85E-03	1	.003
2350	260	840	3.15E-03	1	.007
2400	325	850	5.00E-03	1	.026
2450	382	856	7.80E-03	1	.084
2458	391	858	8.40E-03	1	.096
2420	405	859	9.30E-03	1	.117
2478	415	859	1.00E-02	1	.134
2483	420	860	1.05E-02	1	.137
2485	426	860	1.07E-02	1	.141
2500	437	861	1.21E-02	1	.162
2512	450	862	1.31E-02	1	.170
2520	457	862	1.41E-02	1	.175
2528	465	865	1.50E-02	1	.178
2532	470	865	1.55E-02	1	.179
2550	485	867	1.79E-02	1	.177
2600	528	867	2.63E-02	1	.167
2652	568	870	3.72E-02	1	.159
2695	595	875	5.02E-02	1	.156
2240	623	875	6.40E-02	1	.138
2750	628	875	6.80E-02	1	.134

* A standard card form, IBM electro 888157, is available for punching source statements from this form.

FORTRAN CODING FORM

Program: MASTER DATA FOR JARREL-ASH
Programmer: SEE PROGRAM 1
Date: 5 NOV 64
Page 2 of 14

Form X28-7327-4
Printed in U.S.A.

STATEMENT NUMBER	FORTRAN STATEMENT			
2765	636	880	740E-02	124
2790	650	880	840E-02	105
2800	657	880	900E-02	096
2805	660	881	910E-02	093
2812	662	881	940E-02	085
2850	628	887	116E-01	058
2860	683	889	121E-01	053
2875	688	888	131E-01	044
2880	693	889	133E-01	043
2900	697	890	199E-01	032
2915	703	890	160E-01	030
2922	705	890	167E-01	025
2926	706	890	169E-01	024
2943	712	894	183E-01	021
2966	719	895	205E-01	015
2969	720	895	208E-01	015
2973	722	899	213E-01	014
2990	725	899	228E-01	011
3000	727	900	243E-01	009
3003	728	900	245E-01	008

* A standard card form, IBM electro 888157, is available for punching source statements from this form.

FORTRAN CODING FORM

Form X28-7327-4
Printed in U.S.A.

Program: MR. JR. cont   Page 3 of 14

Programmer: _____ Date: _____

Punching Instructions — Graphic / Punch — Card Form # — Identification

STATEMENT NUMBER		FORTRAN STATEMENT			
3007	749	900	246E-01	1	008
3014	732	900	255E-01	1	008
3017	733	900	258E-01	1	0108
3026	735	900	267E-01	1	007
3055	737	900	303E-01	1	007
3080	742	900	339E-01	1	006
3125	749	900	410E-01	1	002
3130	751	900	418E-01	1	002
3132	752	900	421E-01	1	002
3150	754	900	450E-01	1	001
3158	755	900	460E-01	1	001
2680	585	873	451E-02	2	001
2695	595	875	502E-02	2	003
2740	623	875	640E-02	2	008
2750	628	875	680E-02	2	011
2765	636	880	740E-02	2	015
2790	650	880	840E-02	2	026
2800	657	880	900E-02	2	029
2805	660	881	910E-02	2	030
2812	662	881	940E-02	2	014
2850	670	887	116E-01	2	111

* A standard card form, IBM electro 888157, is available for punching source statements from this form.

34

FORTRAN CODING FORM

Program: M.D., J.A. cont

Programmer:

Page 4 of 14

Punching Instructions — Graphic / Punch

Card Form #

Identification (73–80)

STATEMENT NUMBER				FN	7F
2860	683	888	.121E-01	2	.138
2875	688	888	.131E-01	2	.146
2880	693	889	.133E-01	2	21.2
2900	697	890	.149E-01	2	.260
2915	703	890	.160E-01	2	26.2
2922	705	890	.167E-01	2	.255
2926	706	890	.169E-01	2	25.0
2943	712	894	.183E-01	2	21.2
2966	719	895	.205E-01	2	.197
2969	720	895	.208E-01	3	.194
2923	722	899	.213E-01	2	.191
2980	725	899	.228E-01	2	.176
3000	729	900	.243E-01	2	.166
3003	728	900	.245E-01	2	.164
3007	729	900	.246E-01	2	.158
3014	732	900	.255E-01	2	.151
3017	733	900	.258E-01	2	.148
3026	735	900	.267E-01	2	.136
3055	737	900	.303E-01	2	.096
3080	742	900	.339E-01	2	.056
3125	749	906	.410E-01	2	.033

* A standard card form, IBM electro 888157, is available for punching source statements from this form.

FORTRAN CODING FORM

Form X28-7327-4
Printed in U.S.A.

Program: M.D.-J.A.
Programmer:
Page 5 of 14

Punching Instructions — Graphic / Punch — Card Form #

Identification: 73 — 80

STATEMENT NUMBER	C	7–10	15	20	25 FN	30 TF
3130		751	900	418E-01	2	032
3132		752	900	421E-01	2	020
3158		755	900	460E-01	2	017
3200		760	900	547E-01	2	001
2860		683	888	121E-01	3	010
2875		688	888	131E-01	3	002
2880		693	889	133E-01	3	003
2900		697	890	149E-01	3	004
2915		703	890	160E-01	3	005
2922		705	890	167E-01	3	005
2926		706	890	169E-01	3	006
2943		712	894	183E-01	3	006
2966		719	895	205E-01	3	008
2969		720	895	208E-01	3	011
2973		722	899	213E-01	3	012
2990		725	899	228E-01	3	013
3000		727	900	243E-01	3	015
3003		728	900	245E-01	3	016
3007		729	900	246E-01	3	017
3014		732	900	255E-01	3	021
3017		733	900	258E-01	3	023

* A standard card form, IBM electro 888157, is available for punching source statements from this form.

FORTRAN CODING FORM

Form X28-7327-4
Printed in U.S.A.

Page 6 of 14

Program _____   M.D.J.A. cont

Programmer _____   Date _____

Punching Instructions — Graphic ____ Punch ____ — Card Form # ____

Identification (73–80)

FORTRAN STATEMENT

STATEMENT NUMBER	(7)	10	15	20	25	30
3026	7	35	900	2.67E-01	3	026
3055	7	37	900	3.03E-01	3	050
3080	7	42	900	3.39E-01	3	071
3125	7	49	900	4.10E-01	3	205
3130	7	51	900	4.18E-01	3	220
3132	7	52	900	4.21E-01	3	226
3150	7	54	900	4.50E-01	3	236
3158	7	55	900	4.60E-01	3	236
3200	7	60	900	5.47E-01	3	196
3300	7	72	900	7.90E-01	3	051
3307	7	73	900	8.00E-01	3	046
3315	7	74	900	8.40E-01	3	044
3325	7	75	900	8.25E-01	3	032
3341	7	76	900	9.15E-01	3	028
3355	7	78	900	9.80E-01	3	015
3377	7	80	900	1.03E+00	3	008
3387	7	81	900	1.08E-00	3	007
3400	7	83	900	1.12E 00	3	006
3415	7	84	900	1.19E 00	3	005
3423	7	85	900	1.21E 00	3	004
3445	7	87	900	1.29E 00	3	001

C FOR COMMENT

* A standard card form, IBM electro 888157, is available for punching source statements from this form.

Form X28-7327-4
Printed in U.S.A.

IBM FORTRAN CODING FORM

Program _____   Punching Instructions   Page 7 of 14

Programmer M.D., J.A. cat.   Date ____   Graphic ___ Punch ___   Card Form * ___   Identification 73 __ 80

STATEMENT NUMBER	C	FORTRAN STATEMENT
3450	787	F 9.00 1.31E 00 3.001
3200	760	9.00 5.47E-01 4.00†
3280	768	9.00 7.43E-01 4.012
3300	772	9.00 7.90E-01 4.036
33 05	773	9.00 8.00E-01 4.038
3315	774	9.00 8.40E-01 4.061
3325	775	9.00 8.75E-01 4.086
3341	776	9.00 9.15E-01 4.125
3355	778	9.00 9.80E-01 4.136
3377	780	9.00 1.03E 00 4.146
3387	781	9.00 1.08E 00 4.149
3400	783	9.00 1.12E 00 4.149
3415	784	9.00 1.19E 00 4.146
3423	785	9.00 1.21E 00 4.144
3445	787	9.00 1.29E 00 4.114
3450	787	9.00 1.31E 00 4.106
3500	790	9.00 1.52E 00 4.038
3542	794	9.00 1.22E 00 4.015
3550	795	9.00 1.78E 00 4.012
3559	796	9.00 1.81E 00 4.011
3566	797	9.00 1.87E 00 4.007

* A standard card form, IBM electro 888157, is available for punching source statements from this form.

IBM

FORTRAN CODING FORM

Form X28-7327-4
Printed in U.S.A.

Page 8 of 14

Program: McD. J.A. cont

Punching Instructions — Graphic / Punch — Card Form #

Identification (73–80)

FORTRAN STATEMENT

STATEMENT NUMBER	7					
3600	798	900	205	E 00	4	004
3640	799	900	233	E 00	4	002
3645	800	900	238	E 00	4	001
3450	287	900	131	E 00	5	001
3500	290	900	152	E 00	5	002
3542	294	900	172	E 00	5	010
3550	295	900	178	E 00	5	014
3559	296	900	181	E 00	5	014
3566	297	900	187	E 00	5	017
3600	798	900	205	E 00	5	048
3640	799	900	233	E 00	5	141
3645	800	900	238	E 00	5	153
3650	801	900	241	E 00	5	159
3652	801	900	242	E 00	5	164
3660	801	900	247	E 00	5	176
3666	802	900	250	E 00	5	178
3673	802	900	258	E 00	5	179
3680	803	900	262	E 00	5	179
3700	803	900	276	E 00	5	126
3740	804	900	311	E 00	5	169
3746	804	900	380	E 00	5	163

* A standard card form, IBM electro 888157, is available for punching source statements from this form.

Form X28-7327-4
Printed in U.S.A.

FORTRAN CODING FORM

Program: MO JA, cont

Punching Instructions — Graphic / Punch — Card Form #

Page 9 of 14 — Identification (73–80)

STATEMENT NUMBER	7–10	15	20	25	30
3756	805	900	329E 00	5	162
3764	805	900	340E 00	5	153
3773	805	900	342E 00	5	148
3783	806	900	351E 00	5	134
3793	806	900	361E 00	5	128
3800	806	900	370E 00	5	126
3815	806	900	385E 00	5	118
3825	806	900	395E 00	5	111
3842	807	900	410E 00	5	104
3850	807	900	420E 00	5	099
3860	807	900	430E 00	5	095
3890	808	900	460E 00	5	052
3910	809	900	482E 00	5	025
3950	811	900	520E 00	5	002
3970	811	900	540E 00	5	001
3800	806	900	370E 00	6	001
3815	806	900	385E 00	6	002
3825	806	900	395E 00	6	002
3842	807	900	410E 00	6	004
3850	807	800	420E 00	6	005
3860	807	900	430E 00	6	007

C FOR COMMENT

*A standard card form, IBM electro 888157, is available for punching source statements from this form.

FORTRAN CODING FORM

Program M.D. JA

Programmer

Page 10 of 14

Form X28-7327-4
Printed in U.S.A.

STATEMENT NUMBER	7–10	15	20	25	30
3.890	868	900	460E	00	6 024
3.910	809	900	482E	00	6 055
3.950	811	900	520E	00	6 300
3.925	812	900	545E	00	6 380
3.982	812	900	555E	00	6 391
3.990	813	900	560E	00	6 397
4.014	814	900	580E	00	6 411
4.025	814	900	595E	00	6 414
4.044	815	900	620E	00	6 410
4.050	816	900	630E	00	6 403
4.053	816	900	640E	00	6 400
4.065	816	900	643E	00	6 399
4.077	816	900	660E	00	6 404
4.080	816	900	662E	00	6 411
4.100	817	900	692E	00	6 410
4.110	817	900	718E	00	6 380
4.145	818	900	758E	00	6 120
4.200	819	900	827E	00	6 027
4.250	822	900	918E	00	6 007
4.290	823	900	978E	00	6 001
4.077	816	900	660E	00	7 001

* A standard card form, IBM electro 888157, is available for punching source statements from this form.

IBM

FORTRAN CODING FORM

Program M,O, J,A cnt

Programmer

Punching Instructions

Graphic

Punch

Card Form #

Page 11 of 14

Identification

Form X28-7327-4
Printed in U.S.A.

STATEMENT NUMBER		FORTRAN STATEMENT				
4100	817	900	6.90E 00	7	.002
4110	817	900	7.12E 00	7	0.03
4145	818	900	7.58E 00	7	0.12
4150	818	900	7.60E 00	7	0.13
4200	819	900	8.27E 00	7	2.43
4225	820	900	8.60E 00	7	4.65
4230	821	900	8.70E 00	7	4.65
4250	822	900	9.10E 00	7	4.37
4260	823	900	9.20E 00	7	4.38
4290	823	900	9.78E 00	7	4.84
4360	824	900	9.95E 00	7	4.91
4314	825	900	1.02E 01	7	5.08
4321	825	900	1.03E 01	7	5.08
4352	826	900	1.08E 01	7	5.09
4358	827	900	1.08E 01	7	5.00
4359	827	900	1.09E 01	7	4.98
4364	827	900	1.10E 01	7	4.98
4369	827	900	1.12E 01	7	4.88
4377	828	900	1.13E 01	7	4.82
4400	838	900	1.18E 01	7	4.57
4420	839	900	1.21E 01	7	4.49

* A standard card form, IBM electro 888157, is available for punching source statements from this form.

FORTRAN CODING FORM

Form X28-7327-4
Printed in U.S.A.

Program: M.D., J.A.

Programmer:

Page 12 of 14

STATEMENT NUMBER		FORTRAN STATEMENT				
	7 10	15	20	25	30	
4440	829	900	1.26E	01 7	457	
4450	829	900	1.28E	01 7	456	
4420	830	900	1.32E	01 7	387	
4500	835	900	1.39E	01 7	144	
4510	836	900	1.42E	01 7	160	
4550	838	900	1.51E	01 7	015	
4584	840	900	1.59E	01 7	003	
4601	840	900	1.62E	01 7	002	
4622	842	900	1.69E	01 7	002	
4633	843	900	1.71E	01 7	001	
5046	852	900	2.88E	01 8	001	
5057	852	900	2.91E	01 8	002	
5100	853	900	3.05E	01 8	007	
5150	854	900	3.23E	01 8	025	
5200	855	900	3.40E	01 8	135	
5250	855	900	3.61E	01 8	620	
5263	855	900	3.65E	01 8	655	
5300	855	900	3.78E	01 8	601	
5320	855	900	3.86E	01 8	590	
5350	856	900	3.98E	01 8	603	
5365	856	900	4.02E	01 8	610	

* A standard card form, IBM electro 888157, is available for punching source statements from this form.

FORTRAN CODING FORM

Form X28-7327-4
Printed in U.S.A.

IBM

Program:

Programmer: M.D.S.A.   Date:

Punching Instructions — Graphic / Punch — Card Form # — *

Page 13 of 14

Identification (73–80)

STATEMENT NUMBER	C	FORTRAN STATEMENT					
(1–5)	(6)	(7–10)	(15)	(20)	(25)	(27)	(30)
5376		856	900	407E	01	8	621
5400		856	900	414E	01	8	631
5419		856	900	421E	01	8	631
5430		856	900	424E	01	8	631
5450		856	900	431E	01	8	626
5458		856	900	436E	01	8	621
5461		856	900	438E	01	8	620
5466		856	900	440E	01	8	618
5469		856	900	440E	01	8	617
5479		856	900	442E	01	8	610
5500		856	900	453E	01	8	595
5550		856	900	472E	01	8	558
5580		856	900	486E	01	8	550
5600		856	900	495E	01	8	551
5610		856	900	499E	01	8	550
5650		857	900	515E	01	8	468
5700		857	900	535E	01	8	163
5750		857	900	555E	01	8	039
5770		858	900	562E	01	8	030
5782		858	900	570E	01	8	020
5794		859	900	573E	01	8	016

* A standard card form, IBM electro 888157, is available for punching source statements from this form.

FORTRAN CODING FORM

Form X28-7327-4
Printed in U.S.A.

Program: M.D. J.A.

Programmer:

Page 14 of 14

STATEMENT NUMBER	C	7-10	15	20	25		30
5800		859	900	575,E 01	8		0,15
5850		859	900	592,E 01	8		0,04
5887		859	900	610,E 01	8		0,01
5550		859	900	472,E 01	9		0,01
5600		859	900	495,E 01	9		0,05
5650		859	900	515,E 01	9		0,42
5700		859	900	535,E 01	9		3,28
5720		859	900	542,E 01	9		4,00
5750		859	900	555,E 01	9		4,54
5770		859	900	562,E 01	9		5,00
5782		859	900	570,E 01	9		5,20
5794		859	900	573,E 01	9		5,30
5800		859	900	575,E 01	9		5,40
6820		859	900	580,E 01	9		5,40
5850		859	900	592,E 01	9		5,16
5882		859	900	604,E 01	9		4,67
5893		859	900	610,E 01	9		4,42
5900		859	900	615,E 01	9		3,90
6000		859	900	645,E 01	9		1,10
6050		859	900	660,E 01	9		0,10
6080		859	900	670,E 01	9		0,01

FORTRAN STATEMENT

Punching Instructions — Graphic — Punch — Card Form #

Identification 73 — 80

* A standard card form, IBM electro 888157, is available for punching source statements from this form.

45

IBM

FORTRAN CODING FORM

Form X28-7327-4
Printed in U.S.A.

Program: M.D.J.A. wavelengths not covered by Filters — 29 wavelengths

Programmer: _____ Date: _____

Punching Instructions — Graphic / Punch — Card Form # _____

Page 1 of 2   Identification (73-80)

STATEMENT NUMBER	10	15	20	25	30
4633	842	900	.171E 01	0	.1000
4643	843	900	.174E 01	0	.1000
4664	844	900	.178E 01	0	.1000
4675	844	900	.181E 01	0	.1000
4685	844	900	.183E 01	0	.1000
4727	844	900	.195E 01	0	.1000
4733	844	900	.197E 01	0	.1000
4740	844	900	.199E 01	0	.1000
4763	845	900	.208E 01	0	.1000
4800	845	900	.213E 01	0	.1000
4810	845	900	.216E 01	0	.1000
4820	845	900	.219E 01	0	.1000
4851	846	900	.228E 01	0	.1000
4883	846	900	.237E 01	0	.1000
4893	847	900	.239E 01	0	.1000
4915	848	900	.245E 01	0	.1000
4942	849	900	.252E 01	0	.1000
4958	850	900	.258E 01	0	.1000
4970	851	900	.263E 01	0	.1000
5000	853	900	.271E 01	0	.1000
5017	853	900	.278E 01	0	.1000

* A standard card form, IBM electro 888157, is available for punching source statements from this form.

FORTRAN CODING FORM

IBM

Form X28-7327-4
Printed in U.S.A.

Program: M.D.J.A. wavelengths not covered by Filters

Programmer: _____ Date: _____

Punching Instructions — Graphic _____ Punch _____ — Card Form # _____

Page 2 of 2 Identification 73–80

STATEMENT NUMBER	FORTRAN STATEMENT
5027	853 900 280E 01 0 1000
5037	853 900 284E 01 0 1000
5046	853 900 288E 01 0 1000
5057	853 900 291E 01 0 1000
6100	859 900 670E 01 0 1000
6117	859 900 695E 01 0 1000
6124	859 900 700E 01 0 1000
6130	859 900 702E 01 0 1000

* A standard card form, IBM electro 888157, is available for punching source statements from this form.

APPENDIX B
Master Data for Perkin—Elmer Monochromator Model 99

FORTRAN CODING FORM

APPENDIX B

Program: MASTER DATA MODEL 99
Programmer: SEE PROGRAM 2
Date: 5-NOV-64

Graphic / Punch / Punching Instructions / Card Form # / Page 1 of 8

STATEMENT NUMBER	RM 10	TQ 15	VS 20	25	FN 30	TF 35
534	855	926	388	E+01	8	606
536	855	926	398	E 01	8	610
540	855	926	412	E 01	8	631
543	855	927	422	E 01	8	631
546	855	927	432	E 01	8	626
550	855	927	453	E 01	8	595
553	855	927	462	E 01	8	575
558	855	927	482	E 01	8	555
560	855	927	491	E 01	8	551
561	855	927	499	E 01	8	551
566	856	927	515	E 01	8	472
569	857	927	530	E 01	8	200
573	858	927	542	E 01	8	020
577	858	927	558	E 01	8	030
579	858	927	562	E 01	8	012
583	859	927	580	E 01	8	008
588	859	927	595	E 01	8	001
558	855	927	482	E 01	9	001
560	855	927	491	E 01	9	005
562	855	927	500	E 01	9	010
566	855	927	515	E 01	9	060

C FOR COMMENT

* A standard card form, IBM electro 888157, is available for punching source statements from this form.

IBM

FORTRAN CODING FORM

Form X28-7327-4
Printed in U.S.A.

Program: MODEL 99 MASTER DATA

Page 2 of 8

Statement Number	FORTRAN Statement
569	0008570009R190053DE+010090031000
523	858 927 542E 1 9 414
572	858 927 558E 1 9 490
581	859 928 570E 1 9 540
583	859 928 580E 1 9 5135
582	859 928 595E 1 9 495
595	860 928 620E 1 9 290
597	860 928 630E 1 9 020
600	860 928 645E 1 9 070
604	860 928 652E 1 9 011
608	860 928 660E 1 9 001
587	859 928 595E 1 10 001
592	859 928 615E 1 10 002
595	860 929 620E 1 10 015
604	860 929 652E 1 10 050
644	854 930 844E 1 10 345
670	850 930 928E 1 10 5157
680	848 930 964E 1 10 601
690	846 930 985E 1 10 619
695	846 930 991E 1 10 619
710	842 930 104E 2 10 602

* A standard card form, IBM electro 888157, is available for punching source statements from this form.

IBM

FORTRAN CODING FORM

Form X28-7327-4
Printed in U.S.A.

Program: Model 99 Master Data

Programmer: _____ Date: _____

Punching Instructions — Graphic: ___ Punch: ___ Card Form #: ___

Page 3 of 8

Identification [73 — 80]

STATEMENT NUMBER	C	FORTRAN STATEMENT
720		00825009300107E+020100.0589
740		745 930 114E 2 10 485
253		695 930 120E 2 10 390
790		665 930 132E 2 10 122
800		695 930 134E 2 10 082
820		740 930 137E 2 10 040
850		825 930 141E 2 10 018
863		835 930 142E 2 10 011
900		850 930 144E 2 10 094
909		855 930 145E 2 10 002
955		878 930 146E 2 10 001
670		850 930 928E 1 11 001
680		848 930 960E 1 11 001
710		842 930 104E 2 11 002
253		695 930 120E 2 11 003
770		695 930 124E 2 11 010
800		695 930 134E 2 11 100
820		740 930 137E 2 11 220
850		825 930 141E 2 11 570
863		835 930 142E 2 11 620
871		838 930 142E 2 11 688

IBM

FORTRAN CODING FORM

Form X28-7327-4
Printed in U.S.A.

Program	Model 99 Master Data		Punching Instructions			Page 4 of 8
Programmer	Date	Graphic		Card Form *		Identification
		Punch				73 ____ 80

C FOR COMMENT

FORTRAN STATEMENT

STATEMENT NUMBER	7	10	15	20	25	30
	900000	8520093000145E+02011006L9				
909	855	93	145E	2 11	610
940	868	93	146E	2 11	589
955	878	93	146E	2 11	590
990	885	93	146E	2 11	600
1001	888	93	146E	2 11	650
1010	892	93	145E	2 11	660
1020	894	93	145E	2 11	660
1043	897	93	143E	2 11	640
1070	903	93	142E	2 11	590
1080	904	93	141E	2 11	588
1104	905	93	140E	2 11	580
1125	905	93	138E	2 11	450
1129	905	93	138E	2 11	438
1150	906	93	136E	2 11	230
1180	908	93	134E	2 11	092
1200	910	93	133E	2 11	036
1242	910	93	129E	2 11	012
1265	912	93	127E	2 11	009
1300	913	93	123E	2 11	.007
1345	914	92	117E	2 11	006

* A standard card form, IBM electro 888157, is available for punching source statements from this form.

FORTRAN CODING FORM

IBM

Form X28-7327-4
Printed in U.S.A.

Program: MASTER DATA MODEL 99

Programmer: ____ Date: ____

Punching Instructions — Graphic ____ Punch ____

Card Form # ____

Page 5 of 8

Identification 73 ____ 80

STATEMENT NUMBER	C	FORTRAN STATEMENT
1355		0009150090901116E+02011000106.
1360		915 900 116E 2 11 006
1395		916 761 112E 2 11 006
1410		918 885 110E 2 11 006
1442		922 920 106E 2 11 007
1483		922 930 101E 2 11 009
1510		922 930 925E 1 11 011
1515		922 930 920E 1 11 011
1550		922 930 935E 1 11 016
1592		922 930 872E 1 11 088
1623		922 930 851E 1 11 030
1641		922 930 828E 1 11 028
1625		922 930 795E 1 11 016
1692		922 930 778E 1 11 016
1734		922 930 732E 1 11 011
1260		922 930 708E 1 11 009
1290		922 930 628E 1 11 003
1840		922 930 623E 1 11 003
1906		922 922 565E 1 11 001
1080		904 930 141E 2 12 001
1104		905 930 140E 2 12 003

* A standard card form, IBM electro 888157, is available for punching source statements from this form.

IBM

FORTRAN CODING FORM

Form X28-7327-4
Printed in U.S.A.

Program: MASTER DATA MODEL 99

Programmer _____ Date _____

Punching Instructions — Graphic / Punch — Card Form * _____

Page 6 of 8

Identification 73 — 80

C FOR COMMENT

STATEMENT NUMBER	FORTRAN STATEMENT
1125	0090510093000138E+020012000099.
1129	905 930 138E 2 12 010
1150	906 930 136E 2 12 015
1180	908 930 134E 2 12 040
1200	910 930 133E 2 12 090
1242	910 930 129E 2 12 452
1265	912 930 127E 2 12 680
1280	913 930 125E 2 12 288
1300	913 930 123E 2 12 760
1340	914 925 118E 2 12 204
1395	914 920 112E 2 12 204
1355	915 909 116E 2 12 708
1360	915 900 116E 2 12 710
1395	916 761 112E 2 12 745
1410	918 885 110E 2 12 748
1442	922 920 106E 2 12 707
1460	922 930 104E 2 12 700
1483	922 930 101E 2 12 712
1510	922 930 975E 1 12 735
1515	922 930 920E 1 12 732
1520	922 930 966E 1 12 752

* A standard card form, IBM electro 888157, is available for punching source statements from this form.

FORTRAN CODING FORM

Program: MASTER DATA — MODEL 99

Page 7 of 8

Form X28-7327-4
Printed in U.S.A.

STATEMENT NUMBER	FORTRAN STATEMENT
1550	0009220093000935E+0101200738
1570	922 930 910E 1 12 0758
1597	922 930 872E 1 12 0711
1623	922 930 851E 1 12 0640
1647	922 930 828E 1 12 0580
1675	922 930 795E 1 12 0522
1692	922 930 778E 1 12 0560
1734	922 930 732E 1 12 0645
1760	922 930 708E 1 12 0590
1790	922 930 678E 1 12 0360
1840	922 930 623E 1 12 0090
1865	922 929 600E 1 12 0050
1900	922 926 565E 1 12 0026
1930	922 926 541E 1 12 0015
1960	922 926 519E 1 12 0012
1970	922 926 510E 1 12 0018
2025	922 920 472E 1 12 0005
2092	922 895 431E 1 12 0001
2155	922 826 398E 1 00 1000
2193	922 260 380E 1 00 1000
2210	922 450 324E 1 00 1000

Form X28-7327-4
Printed in U.S.A.

IBM

FORTRAN CODING FORM

Program: MASTER DATA – MODEL 99

Programmer ____ Date ____

Punching Instructions

| Graphic | | | | Card Form # | * |
| Punch | | | | | |

Page 8 of 8

Identification (73 – 80)

STATEMENT NUMBER (1–5)	C (6)	FORTRAN STATEMENT (7–72)
23050		922 825 331E+01 00 1000
22700		922 550 346E+01 00 1000

* A standard card form, IBM electro 888157, is available for punching source statements from this form.

APPENDIX C
Report of Calibration of the Spectral-Directional Reflectance of Two Front-Surface Aluminum Mirrors

U.S. Department of Commerce
National Bureau of Standards
Washington, D.C. 20234

National Bureau of Standards

182815

REPORT OF CALIBRATION
on the
Spectral Directional Reflectance
of
Two Front-Surface Aluminum Mirrors

Submitted by
The Eppley Laboratory, Inc.
Newport, Rhode Island

(See Purchase Order No. 1532, Requisition No. 6022, dated October 13, 1964, signed by Mr. George L. Kirk.)

1. Purpose.

The purpose of this test is the measurement of the spectral directional reflectance of two front-surface aluminum mirrors over the spectral range 0.26 to 2.5 microns.

2. Materials.

The two front-surface aluminum mirrors were submitted for measurement by The Eppley Laboratory, Inc., and were received on October 14, 1964. Each mirror is approximately 3.7 by 3.2 centimeters in size and approximately 1.2 centimeters in thickness. The two specimens had no identifying marks when received and have therefore been marked "1" and "2" on the side in pencil for correlation with the curves. The specimen "2" was apparently damaged in shipment and had a large blemish near the center when received.

3. Measurements.

Measurements of spectral directional reflectance were made relative to a MgO reference surface prepared on October 13, 1964, by means of a Cary Model 14 recording spectrophotometer equipped with a model 1411 integrating sphere reflectance attachment and a linear (0% to 100% full scale) slidewire. Measurements were made for the condition of included specular component. The following source-detector combinations were used for the indicated wavelength ranges:

(1) 0.26 to 0.4 micron, hydrogen source and RCA 6217 end-on multiplier phototube detector; (2) 0.35 to 0.75 micron, tungsten source and RCA 6217 end-on multiplier phototube detector; and (3) 0.6 to 2.3 microns, tungsten source and lead sulfide detector. Two modes of illumination of the specimen are used to cover this wavelength range. In Type I mode, used for the spectral range 0.26 to 0.75 micron ((1) and (2) above), the specimen is illuminated with

monochromatic flux and the reflected flux is viewed diffusely. In Type II mode, used for the spectral range 0.6 to 2.5 microns ((3) above), the specimen is profusely illuminated with nondispersed flux and the reflected flux viewed at an angle of approximately 6° from the normal to the specimen surface. The slit widths varied over the spectral range of interest from less than 1 nanometer to approximately 9 nanometers (formerly called millimicrons) of spectral width. Check measurements of spectral directional reflectance were made by means of a General Electric recording spectrophotometer equipped with slits approximating 10 nanometers of spectral width for the visible spectral region 0.4 to 0.75 micron. These measurements were also for the condition of included specular component.

4. Results.

The results of the measurements of spectral directional reflectance are recorded automatically during the wavelength scan, and are shown on the enclosed Ozalid copies of the original recordings (Cary 173-558/1 to -558/15, and GE II—3180).

5. Remarks.

The following method of data reduction should be used. The curves of spectral directional reflectance of the specimens should be read together with the curves for the 100% curve and 0% curve at the wavelengths of interest. The 100% curves, measured at the beginning and end of each series of measurements, should be averaged. The value of the 0% curve should be subtracted from the data of the specimens and the average 100% curve. The zero corrected data of the specimens should then be divided by the zero corrected data of the 100% curve. It will be noted that the data on the specimens, obtained in the visible and ultraviolet spectral regions, while they agree with each other at the overlap wavelengths, are higher than the data obtained for the infrared spectral region. This disagreement is due to the geometry of the integrating sphere and the differences in the two modes of illuminating and viewing the specimen used to cover the entire spectral range. The data obtained in the infrared are believed to be correct and the data for the visible and ultraviolet spectral regions should be adjusted to agree with the infrared data.

If it is desired to reduce the data obtained by means of the GE recording spectrophotometer, there are enclosed 2 computation sheets for this purpose, the column headings of which explain the steps to be taken to obtain data relative to freshly prepared MgO.

In accord with your Dr. A. J. Drummond's telephone conversation of October 15, 1964 with our Mr. Schleter, the specimens and a copy of the report and the spectrophotometer curves are being forwarded for his attention at the Jet Propulsion Laboratory, Pasadena, California.

For the Director,
L. E. Barbrow, Chief
Photometry & Colorimetry Section
Metrology Division

* * A true copy * *

APPENDIX D

Memorandum on Eppley Spectral Measurement[D-1]

Beginning Monday, October 19, 1964, the Eppley Laboratory will measure the spectrum in the JPL 25-foot space simulator. During this measurement J. Gatewood, J. Jolley, and I will assist Dr. A. J. Drummond and John Hickey of the Eppley Laboratory.

The purpose of this measurement is as follows:

1. To define the solar spectrum in the 25-foot space simulator.

2. To correlate vacuum-air sun at 1 earth constant.

3. To determine spectral repeatability at different flux levels (2 levels).

4. To ascertain spectral beam uniformity with respect to position across a plane (3 pts).

5. To get an "on the spot" correlation-calibration of the MK IV as referenced to the monochromator.

6. To ascertain a reference spectrum which can be periodically checked with the MK IV.

7. To investigate other filters which might be more appropriate for usage in the 25-foot space chamber.

To accomplish these purposes, the following has been done:

1. A Corning, U.V. grade, 7940 SiO_2 transfer window has been purchased. This window has a transmittance of 75% + at .2 microns and levels out at 92% + at .26 microns for 10 mm thickness. (Note: These numbers include Fresnel reflections). The window is $\frac{5}{8}''$ thick by 8'' in diam. which yields a safety factor of 9.5 assuming usage of full aperture (8'') and free edges. This is assuming a modulus of rupture, abraded at 25°C of 7000+ #/in.^{2}. Assuming the more realistic case in which the edges are "clamped" (by the O ring) at a free diameter of $6\frac{1}{2}''$ the safety factor is 23.5. This window will be calibrated for spectral transmission in position with the monochromator. The purpose in relating the safety information here is to aid in relinquishing anxiety over working in the immediate area of the window.

2. Concave spherical Pyrex mirrors of focal length = 75 cm were obtained to yield a fairly uniform field in the test area which is approximately 7 feet removed from the astigmatic image of the solar sun produced by the mirror. The mirror will be temperature controlled.

3. The Eppley MK IV spectral radiometer has been modified with a fast-response detector ($\approx$ 3 sec in vac.)

4. Eppley has assembled the following equipment

   a. The Eppley MK V radiometer with 4 sets of filter wheels ($\approx$ 50 filters).

[D-1]This is a true copy of an interoffice memorandum from T. E. Gindorf, Jet Propulsion Laboratory, dated October 12, 1964, which outlines the tests to be undertaken by the Eppley Laboratory, as understood at that time.

b. The Perkin-Elmer Model 99 monochromator to be used with a quartz (also possibly Na Cl for I.R.) prism.

c. A Jarrell Ash grating monochromator.

The configuration of equipment is illustrated in Figure 1. John Gatewood is assembling the equipment needed to perform these measurements and will have everything prepared by October 18, 1964.

The following is a list of the preparatory events which precede that date.

1. Optics, vacuum, and chamber coldwall system must be fully operational.

2. Adequate vacuum instrumentation fully installed and checked out.
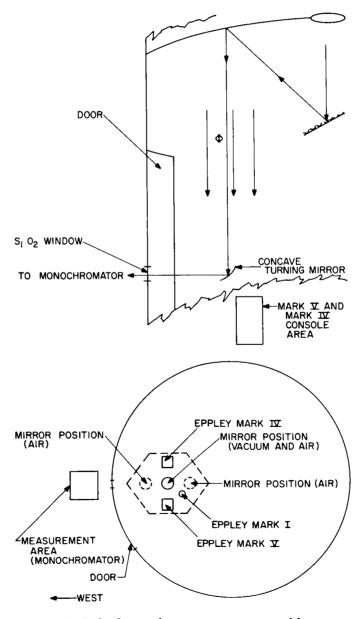

Fig. D-1. Spectral measurement assembly

3. Eppley MK IV in position and ready for operation. Console, etc., wired up and checked out.

4. Ladder stand for Eppley MK V in position with adjustable ball joint fixture installed and ready to accept the instrument when it arrives.

5. Chamber ladder stand for spherical turning mirror should be in position on guide rails for locating in different areas of the solar beam. Thermocouples should be installed on the coolant line and on the holding fixture (coil cooled plate). The mounting fixture to the ladder should be an adjustable ball joint.

6. SiO_2 U.V. grade window installed. (This will have to be done on the 19th of October).

7. Eppley MK I with iris control solar cell installed.

8. Table arrangement for supporting monochromators positioned on the door platform.

9. Two tables for MK IV and MK V consoles on the door apron (east of door controls).

10. All cables in position and through feed throughs.

11. Short circuited solar cell wand for spot mapping available.

12. N_2 bottle at monochromator area for pressurizing model 99 monochromator if needed.

13. At least 6 spare thermocouples available in chamber for attachment in undefined areas.

14. The floor grating in the solar beam should be removed.

15. Turning mirrors for monochromator and standard lamps should be mounted on adjustable stable stands.

16. 110-120 V 60 cycle AC power outlets available to MK V-MK IV and monochromator areas.

This measurement and the inherent unknowns in such things as alignments, measurements, etc., necessitate a flexible attitude. For example, it is not possible to say exactly when the chamber will be pumped down or when the lights should be turned on, etc. However, the following test plan which reflects the flexible nature of events is the outline to be followed. There will be no slant board prepared due to the nature of the measurement.

The following discussion defines the simulator conditions under which the spectrum will be measured beginning October 18, 1964. The test plan presented below is to be the definition of which measurements will be taken and what is expected to be the resultant form of the data. It is anticipated that much of the data can be reduced during the week of the measurements with the aid of several of the JPL people and a computer.

Sunday, October 18, 1964 — Arrive at LAX and have equipment sent to JPL. On arrival of equipment at JPL, the instrumentation-hardware interface can be checked for compatibility, i.e., all equipment can be assembled for check runs and alignment on Monday.

Monday, October 19, 1964 — 0800-1200 check out, setup, and prepare for air instruments. 1300 — make air measurements of the spectrum with the turning mirror at the back edge of the solar beam at 134 watts/ft.[2] Two runs are to be made with the monochromator arrangement at this location. The MK IV and MK V will be run at the same time as the monochromator. The MK IV and MK V will be situated in a fixed position throughout all measurements, namely near the center of the beam. Make a run without the SiO_2 window in position.

Tuesday, October 20, 1964 — 0800-1200 — Relocate the solar beam turning mirror near the front edge of the solar beam. Make air measurement at 134 w/ft.[2] Make two runs at this location with the monochromator. Make a run without the SiO_2 window in position. NOTE: The MK IV and MK V will be run at the same time as the monochromator and at the same location as above. Relocate mirror at center of beam and repeat tests as described at the front edge of the beam. At this location 2 runs also need to be made without the SiO_2 window in position. 1300 — Continue measurements.

Wednesday, October 21, 1964 — 0800-1200 Completion of air measurements. 1300 — Reduce data. Prepare for vacuum measurement. During the night on completion of these measurements, the chamber will be evacuated and all equipment must be secured for operations under vacuum and coldwall conditions prior to leaving the Lab for the day.

Thursday, October 22, 1964 — 0800-1200 Vacuum measurements at levels of 134 w/ft^{2} and 51 w/ft^{2} will be made. Three scans will be made at each level with the monochromator arrangement. The MK IV and MK V will be making measurements at the same time. 1300 — Continue as needed.

Friday, October 23, 1964 — 0800 — Continue as required above.

A complete report which will include the following must be received by November 30, 1964.

1. All original data

2. All data is to be reduced to continuous graphs of the form of percentage of total spectral energy versus wavelength.

3. Interpretation of the spectrum in the system

   a. Beam spectral uniformity (3 position air measurements)

   b. Spectral reproducibility (2 flux level vacuum measurements)

4. Comparison of the spectrum with the Johnson and Nicolet curves.

5. Comparison of the air to vacuum measurements.

In summary, there will be measurements made at 3 positions at one flux level in air, measurements made at two flux levels in vacuum. The number of scans desired are listed as mutually agreed upon minimums (telecons — Gindorf and Hickey). The SiO_2 window required to transmit the solar energy out of the chamber will be calibrated in position at JPL.

This concludes the test outline as seen at this time. Revisions may occur as required but they must have the approval of the JPL cognizant engineer on this test. In the event extra time and/or money are required to complete this test plan, authorization will have to be acquired at that time.

(Signed)   T. E. Gindorf

APPENDIX E

Supplementary Data

A comparison of the solar spectrum[E-1] with data for the case of one solar constant in vacuum (10^{-6}-torr range) is presented in Table E-1, as follows:

[E-1]See Johnson, F. S., "The Solar Constant," *Journal of Meteorology*, Vol. II, No. 6, December, 1954, pp. 431–439.

Table E-1. Absorptance of various spacecraft materials

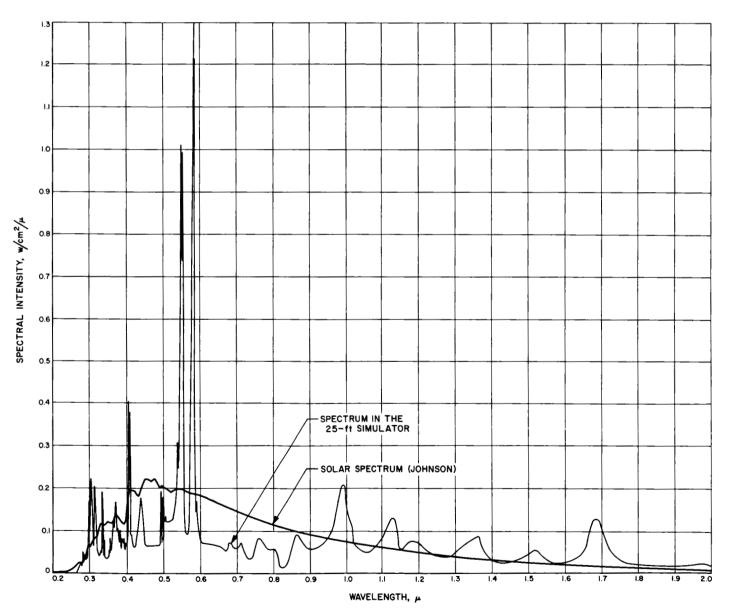| Source	Flat green paint	Flat black paint	White paint	Gold	Solar cell
Solar	0.716	0.95	0.317	0.283	0.765
25-ft simulator	0.672	0.95	0.306	0.249	0.755
Error (%) in absorbed energy	−6.1	0	−3.4	−12.0	−1.2

Fig. E-1. Spectral comparison of solar and 25-ft simulator lamp energy at energy ratio 1:1